Ligand Electronic Effects in Asymmetric Catalysis: Enhanced Enantioselectivity in the Asymmetric Hydrocyanation of Vinylarenes

Albert L. Casalnuovo,* T. V. RajanBabu,*,† Timothy A. Ayers,‡ and Timothy H. Warren§

Contribution No. 6885 from the DuPont Central Research and Development, E328 Experimental Station, Wilmington, Delaware 19880-0328

Received April 28, 1994®

Abstract: The enantioselectivity of the nickel-catalyzed, asymmetric hydrocyanation of vinylarenes using glucose-derived, chiral phosphinite ligands, **L**, increases dramatically when the ligands contain electron-withdrawing *P*-aryl substituents. The substrate and solvent also strongly influence the enantioselectivity, with the highest ee's (85–91% for 6-methoxy-2-vinylnaphthalene (MVN)) obtained for the hydrocyanation of electron-rich vinylarenes in a nonpolar solvent such as hexane. Mechanistic studies suggest the catalytic cycle consists of an initial HCN oxidative addition or vinylarene coordination to "NiL", followed by insertion to form an (η^3-benzyl)nickel cyanide complex, and irreversible reductive elimination of the nitrile. A kinetic analysis of the $NiL_a(COD)$ (L_a, *P*-aryl = 3,5-$(CF_3)_2C_6H_3$) catalyzed hydrocyanation of MVN indicates that as the HCN concentration is increased the catalyst resting state shifts from $NiL_a(COD)$ to a complex containing both MVN and HCN, presumably the (η^3-benzyl)nickel cyanide intermediate $NiL_a(\eta^3\text{-}CH_3CHC_{10}H_6OCH_3)CN$. A ^{31}P NMR analysis of the intermediate $NiL_a(MVN)$ shows little ground state differentiation of the MVN enantiofaces and suggests that the enantioselectivity is determined later in the mechanism. Deuterium labeling studies suggest that *electron-withdrawing P*-aryl substituents increase the rate of reductive elimination of the product nitrile from the (η^3-benzyl)nickel cyanide intermediate and, on this basis, a rationale for the ligand electronic effect is proposed.

Introduction

Strategies for controlling regio- or stereoselectivity in catalytic reactions have usually relied on the design or manipulation of the catalyst *steric* environment,[1] even though the *electronic* properties of ligands can have profound effects on the selectivity and rates of fundamental organometallic processes.[2] In asymmetric catalysis, the manipulation of ligand electronics has seldom been successfully exploited, and in the limited number of cases that have been studied, the underlying reasons for the dependence of enantioselectivity on ligand electronics are poorly understood.[3,4] A better understanding of the origins of these effects should have important implications for organometallic reaction mechanisms and also for the design of better catalysts. Toward this end, we

† Current address: Department of Chemistry, The Ohio State University, 120 West 18th Ave, Columbus, OH 43210.

‡ Current address: Marion Merrell Dow Research Institute, 2110 East Galbraith Road, Cincinnati, Ohio 45215.

§ Current address: Department of Chemistry, MIT, 77 Massachusetts Avenue, Cambridge, MA 02139.

® Abstract published in *Advance ACS Abstracts,* September 1, 1994.

(1) For recent examples see: (a) Trost, B. M.; Van Vranken, D. L.; Bingel, C. *J. Am. Chem. Soc.* **1992**, *114*, 9327–9343. (b) Bao, J.; Wulff, W. D.; Rheingold, A. L. *J. Am. Chem. Soc.* **1993**, *115*, 3814–3815. (c) Corey, E. J.; Noe, M. C. *J. Am. Chem. Soc.* **1993**, *115*, 12579–12580 and references cited therein.

(2) (a) Kubota, M.; Kiefer, G. W.; Ishikawa, R. M.; Bencala, K. E. *Inorg. Chim. Acta* **1973**, *7*, 195–202. (b) Ugo, R.; Pasini, A.; Fusi, A.; Cenini, S. *J. Am. Chem. Soc.* **1972**, *94*, 7364–7370. (c) Thompson, W. H.; Sears C. T., Jr. *Inorg. Chem.* **1977**, *16*, 769–774. (d) Wilson, M. R.; Woska, D. C.; Prock, A.; Giering, W. P. *Organometallics* **1993**, *12*, 1742–1752. (e) Wilson, M. R.; Liu, H.; Prock, A.; Giering, W. *Organometallics* **1993**, *12*, 2044–2050. (f) Akermark, B.; Johansen, H.; Roos, B.; Wahlgren, U. *J. Am. Chem. Soc.* **1979**, *101*, 5876–5883. (g) Tatsumi, K.; Hoffmann, R.; Yamamoto, A.; Stille, J. K. *Bull. Chem. Soc. Jpn.* **1981**, *54*, 1857–1867. (h) Schenkluhn, H.; Berger, R.; Pittel, B.; Zähres, M. *Transition Met. Chem.* **1981**, *6*, 277–287. (i) Tatsumi, K.; Nakamura, A.; Komiya, S.; Yamamoto, A.; Yamamoto, T. *J. Am. Chem. Soc.* **1984**, *106*, 8181–8188. (j) Kraft, G.; Kalbas, C.; Schubert, U. *J. Organomet. Chem.* **1985**, *289*, 247–256. (k) Low, J. J.; Goddard, W. A. III. *J. Am. Chem. Soc.* **1986**, *108*, 6115–6128. (l) Berger, R.; Schenkluhn, H.; Weimann, B. *Transition Met. Chem.* **1981**, *6*, 272–277. (m) Halpern, J.; Okamoto, T. *Inorg. Chim. Acta* **1984**, *89*, L53–L54. (n) Unruh, J. D.; Christenson, J. R. *J. Mol. Catal.* **1982**, *14*, 19–34. (o) Faller, J. W.; Nguyen, J. T.; Ellis, W.; Mazzieri, M. R. *Organometallics* **1993**, *12*, 1434–1438. Substrate electronic effects can also be important; see: (p) Mendez, N. Q.; Seyler, J. W.; Arif, A. M.; Gladysz, J. A. *J. Am. Chem. Soc.* **1993**, *115*, 2323–2334.

(3) Ligand electronics had a pronounced effect on the enantioselectivity of an asymmetric, catalytic alkene epoxidation reaction and an asymmetric, catalytic ketone hydrosilylation reaction; see: (a) Jacobsen, E. N.; Zhang, W.; Guler, M. L. *J. Am. Chem. Soc.* **1991**, *113*, 6703–6704. (b) Nishiyama, H.; Yamaguchi, S.; Kondo, M.; Itoh, K. *J. Org. Chem.* **1992**, *57*, 4306–4309. Until recently (see ref 4c), only modest effects were observed in the asymmetric hydrogenation reaction; see: (c) Morimoto, T.; Chiba, M.; Achiwa, K. *Chem. Pharm. Bull.* **1993**, *41*, 1149–1156. (d) Morimoto, T.; Chiba, M.; Achiwa, K. *Chem. Pharm. Bull.* **1992**, *40*, 2894–2896. (e) Hengartner, U.; Valentine D., Jr.; Johnson, K. K.; Larscheid, M. E.; Pigott, F.; Scheidl, F.; Scott, J. W.; Sun, R. C.; Townsend, J. M.; Williams, T. H. *J. Org. Chem.* **1979**, *44*, 3741–3749. (f) Werz, U.; Brune, H. *J. Organomet. Chem.* **1989**, *365*, 367–377.

(4) (a) RajanBabu, T. V.; Casalnuovo, A. L. *J. Am. Chem. Soc.* **1992**, *114*, 6265–6266. (b) RajanBabu, T. V.; Casalnuovo, A. L. *Pure Appl. Chem.* **1994**, *66*, 1535–1542. (c) RajanBabu, T. V.; Ayers, T. A.; Casalnuovo, A. L. *J. Am. Chem. Soc.* **1994**, *116*, 4101–4102. (d) RajanBabu, T. V.; Ayers, T. A. *Tetrahedron Lett.* **1994**, *35*, 4295–4298.

(5) The highest reported selectivity is 40% ee in a low-yielding hydrocyanation of norbornene. The substrate scope has also been primarily limited to norbornene derivatives; see: (a) Elmes, P. S.; Jackson, W. R. *Aust. J. Chem.* **1982**, *35*, 2041–2051. (b) Hodgson, M.; Parker, D.; Taylor, R. J.; Ferguson, G. *Organometallics* **1988**, *7*, 1761–1766. (c) Baker, M. J.; Pringle, P. G. *J. Chem. Soc., Chem. Commun.* **1991**, 1292–1293.

(6) To the best of our knowledge only one metal-catalyzed asymmetric C–C bond forming reaction is currently practiced on an industrial scale. This is the Cu-catalyzed cyclopropanation of isobutylene (Aratani, T. *Pure App. Chem.* **1985**, *57*, 1839–1844) using ethyl diazoacetate. Several important variants of this reaction have also appeared recently, see: Evans, D. A.; Woerpel, K. A.; Hinman, M. M.; Faul, M. M. *J. Am. Chem. Soc.* **1991**, *113*, 726–728. Lowenthal, R. E.; Abiko, A.; Masamune, S. *Tetrahedron Lett.* **1990**, *31*, 6005–6008. Müller, D.; Umbricht, G.; Weber, B.; Pfaltz, A. *Helv. Chim. Acta* **1991**, *74*, 232–240. A cyclic dipeptide-catalyzed HCN addition to aromatic aldehydes (Oku, J.; Inoue, S. *J. Chem. Soc., Chem. Commun.* **1981**, 229–230) and an amine-mediated ketene–olefin cycloaddition (Wynberg, H.; Staring, E. G. J. *J. Am. Chem. Soc.* **1982**, 104, 166–168) are notable examples of nonmetal-mediated enantioselective C–C bond forming reactions that have been carried out in large scales. Among the hundreds of reactions that have been reported, carbonyl additions of organo zinc reagents (Noyori, R.; Kitamura, M. *Angew. Chem., Int. Ed. Engl.*, **1991**, *30*, 49–69. Schmidt, B.; Seebach, D. *Angew. Chem., Int. Ed. Engl* **1991**, *30*, 99) and the Au(I)-catalyzed additions of isonitriles (Ito, Y.; Sawamura, M.; Hayashi, T. *J. Am. Chem. Soc.*, **1986**, *108*, 6405–6406) have considerable potential for being practical. Takaya's recent results on hydroformylation (Sakai, N.; Mano, S.; Nozaki, K.; Takaya, H. *J. Am. Chem. Soc.* **1993**, *115*, 7033–7034) should prompt further work on this venerable reaction, which in the past was plagued by low catalyst turnover and/or low selectivity.

0002-7863/94/1516-9869$04.50/0

have chosen to study ligand electronic effects in the nickel-catalyzed asymmetric hydrocyanation of alkenes.[4a,b]

We were initially interested in the asymmetric hydrocyanation reaction for three reasons: (a) traditional chiral ligands had been ineffective,[5] (b) truly practical asymmetric carbon–carbon bond forming reactions are rare,[6] and (c) this reaction provides a potentially versatile route to chiral nitriles, amines, and acids.[7] During this study, we discovered a remarkable catalyst electronic effect in the nickel-catalyzed asymmetric hydrocyanation of certain vinylarenes using chiral, bidentate phosphinite ligands, **L**, derived from glucose (eq 1).[4a,b] In this readily modified ligand

$$ArCH{=}CH_2 + HCN \xrightarrow[\text{Catalyst = NiL}]{} ArCH(CH_3)CN \qquad (1)$$

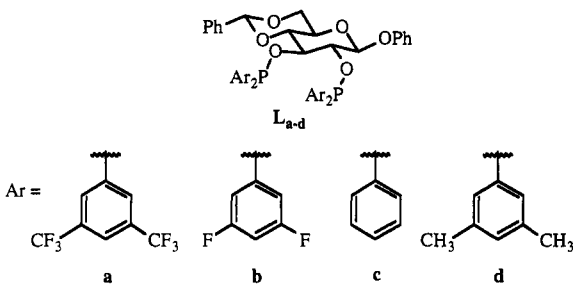

system, the presence of electron-withdrawing, *P-m*-aryl substituents dramatically enhanced the enantioselectivity of the reaction. For example, the ee (enantiomeric excess) of the nickel-catalyzed hydrocyanation of MVN (6-methoxy-2-vinylnaphthalene), a precursor to the anti-inflammatory drug naproxen, increased from 16% to 85% when the dimethyl ligand derivative $\mathbf{L_d}$ was replaced with the trifluoromethyl derivative $\mathbf{L_a}$. Since our initial communication[4a] we have sought to clarify several aspects of this unusual catalyst system, such as the substrate scope, the generality of the electronic effect, and some details of the reaction mechanism. Here we report the results of those efforts, including some insights into how the *P*-aryl substituents affect the fundamental reaction steps.

Results and Discussion

Substrate and Ligand Studies. We examined the asymmetric hydrocyanation of a variety of vinylarenes using the *meta*-substituted ligands $\mathbf{L_{a-d}}$ and some related *ortho*- and *para*-substituted ligands to assess the generality of the ligand electronic effect and the effect of the substrate and solvent on the enantioselectivity. These scouting reactions were carried out by the dropwise addition of an HCN solution to a solution of the vinylarene and, typically, 1–5 mol % of the nickel catalyst at ambient (~25 °C) temperature. The nickel catalysts were synthesized *in situ* by stirring a solution of the ligand with 1 equiv of $Ni(COD)_2$ (COD = 1,5-cyclooctadiene) for several minutes at ambient temperature under a nitrogen atmosphere. Enantiomeric excesses were determined by HPLC analysis of the product nitriles using Daicel Chiralcel OJ or OB columns.[8] Only branched nitriles were detected in these scouting reactions and in subsequent preparative hydrocyanations of MVN and *p*-isobutylstyrene, thus the asymmetric hydrocyanation is completely regioselective.[9] The nitriles obtained from the hydrocyanation of MVN and 4-isobutylstyrene were enriched in the *S* enantiomer as shown by comparison to authentic samples prepared from (*S*)-naproxen and (*S*)-ibuprofen via dehydration of the respective amides. The absolute configurations of the other nitriles in this study were not determined, however, the same major enantiomer was obtained irrespective of the ligand used. We conclude, therefore, that the sense of product chirality is dictated soley by the carbohydrate backbone and that the *S* nitrile is always the major enantiomer when ligands of type **L** are employed.

The results from these hydrocyanation reactions are shown in Tables 1–4. For the ligands $\mathbf{L_{a-d}}$, the ee's increase in the order of increasing substituent electron-withdrawing power $\mathbf{L_d} < \mathbf{L_c} <$

Table 1. Hydrocyanation of Vinylarenes Using Ligands $\mathbf{L_{a-d}}$[a]

		EE(%)			
	Substrate	$\mathbf{L_a}$	$\mathbf{L_b}$	$\mathbf{L_c}$	$\mathbf{L_d}$
1.	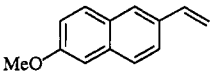	85-91[b]	78[c]	35[d]	16[d]
2.	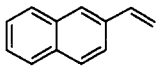	77	75	46[d]	25[d]
3.	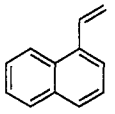	68	—	63	—
4.	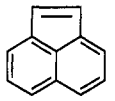	59	—	0	—
5.	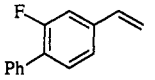	55	—	10[d]	—

[a] 0.10–0.20 M alkene, 1.0–5.0 mol % $Ni(COD)_2/\mathbf{L}$ in hexane. [b] 91% at 0 °C in heptane. [c] Toluene. [d] Benzene.

Table 2. Hydrocyanation of 4-Styrene Derivatives[a]

		EE (%)		
entry	4-substituent	$\mathbf{L_a}$	$\mathbf{L_b}$	$\mathbf{L_c}$
1	CH_3	70	47	1
2	Ph	68	41	8
3	$(CH_3)_2C{=}CH$	63		
4	PhO	60	38	7
5	$(CH_3)_2CHCH_2$	56	38	6
6	CH_3O	52	39	6
7	Cl	40		
8	F	28	15	4
9	CF_3	14	9	1

[a] 0.65 mmol alkene, 0.020 mmol $Ni(COD)_2$, 0.020 mmol ligand, 0.65 mmol HCN in 5 mL of hexane after 24 h.

Table 3. $NiL(CO)_2$ Carbonyl Stretching Frequencies and the Enantiomeric Excesses Obtained for **L** in MVN Hydrocyanation

aryl substituents in **L**	A_1 (cm^{-1})[a]	B_1 (cm^{-1})[a]	ee (%)[b]
3,5-$(CF_3)_2$, $\mathbf{L_a}$	2038	1987 (br)	85–91
3,4,5-F_3	2034	1983	61
3,5-F_2, $\mathbf{L_b}$	2031	1974 (br)	77[c]
3,5-Cl_2	2030	1975	64
4-CF_3	2024	1968	65
4-F	2015	1965	38
H, $\mathbf{L_c}$	2012	1947[d]	35[c]
2-CH_3	2007	1947	0
3,5-$(TMS)_2$	2006	1950	16
3,5-$(CH_3)_2$, $\mathbf{L_d}$	2006	1944[e]	16[c]
2,5-$(CH_3)_2$	2005	1946	9
4-CH_3O	2004	1945	17

[a] Symmetry approximated as C_{2v}. [b] 0.10–0.20 M MVN, 1–6 mol % $Ni(COD)_2/\mathbf{L}$, hexane. [c] Benzene. [d] Shoulder at 1955 cm^{-1}. [e] Shoulder at 1960 cm^{-1}.

(7) Profen drugs, such as naproxen and ibuprofen, can be obtained by hydrolysis of 2-arylpropionitriles to 2-arylpropionic acids.

(8) Enantiomeric excesses obtained from the hydrocyanation of MVN were further supported by optical rotation measurements.

(9) For MVN and *p*-isobutylstyrene, authentic samples of the corresponding linear nitriles were used to verify the regioselectivity; see: (a) Nugent, W. A.; McKinney, R. J. *J. Org. Chem.* **1985**, *50*, 5370–5372. For the other substrates reported here we did not find evidence for the linear nitrile in the ^1H NMR spectra of the isolated nitriles or in the GC analyses of the reaction mixtures (both flame ionization and nitrogen/phosphorus detectors were used).

Table 4. Asymmetric Hydrocyanation Solvent Effects[a]

solvent	ee (%)		
	L_a	L_c	L_d
hexane	85–91 (MVN)[b]		43 (2-VN)
benzene	78 (MVN)	46 (2-VN)	25 (2-VN)
THF	65 (MVN)		
CH_3CN	27 (MVN)	12 (2-VN)	

[a] 0.10–0.20 M alkene, 1–5 mol % $Ni(COD)_2$/L. [b] The same results have been obtained in C_6F_6.

$L_b \leq L_a$ (for L_d–L_a, σ_m = –0.07, 0, 0.34, 0.43),[10] and in most cases, the overall increase is quite marked. Similar to the striking results obtained with MVN, for example, employing the unsubstituted phenyl derivative L_c in the hydrocyanation of acenaphthalene or 4-methylstyrene produced racemic products, whereas the trifluoromethyl derivative L_a gave ee's of 59% and 70%, respectively (Table 1, entry 4; Table 2, entry 1). We also note that the electronic effect is not limited to substitution at the *meta* position as shown by the effect of the related *p*-methoxy (17% ee), fluoro (38% ee), and trifluoromethyl (65% ee) ligand derivatives on the hydrocyanation of MVN (Table 3, column 4). The enantioselectivities are strongly substrate dependent, with ee's as high as 85–91% for MVN (Table 1, entry 1) and as low as 14% for 4-(trifluoromethyl)styrene (Table 2, entry 9). Results from the hydrocyanation of a series of *para*-substituted styrene derivatives, shown in Table 2, suggest a trend between *substrate* electron-donating substituents and higher ee (cf entries 1–6 vs 7–9), although this trend does not strictly correlate with σ_p values. As shown in Table 4, the enantioselectivity also shows a marked dependence on solvent, with nonpolar solvents such as hexane or C_6F_6 giving the highest ee's. The enantioselectivity of MVN hydrocyanation with L_a, for example, drops from 85% ee to 27% ee when acetonitrile is used instead of hexane.

Reaction Mechanism and Catalyst Composition. There are a number of key issues surrounding the mechanism of the NiL-catalyzed hydrocyanation of vinylarenes: the nature of the organometallic species in the catalytic loop, the catalyst resting state, the rates of interconversion of the various diastereomers, and how the *P*-aryl substituents alter the individual rates and hence the overall reaction mechanism. On the basis of the extensive studies reported for the triaryl phosphite–nickel complex catalyzed hydrocyanation of alkenes[11,12] and our own findings for the asymmetric hydrocyanation of vinylarenes (vide infra), we propose the general catalytic cycle shown in Scheme 1 for the $Ni(COD)_2$/L/MVN system. This simplified catalytic cycle is meant to encompass the various diastereomeric pathways generated by the ligand C_1 symmetry.

The formation of the catalyst precursor NiL(COD) (**1**), depicted in the first step, was observed by ^{31}P and ^1H NMR spectroscopy of the L_a and L_c systems. This same complex (L = L_a) was the only species observed by ^{31}P NMR spectroscopy after the NiL_a(COD)-catalyzed hydrocyanation of MVN was complete. Attempts to detect other intermediates during the NiL_a(COD)-catalyzed hydrocyanation of MVN by ^{31}P NMR spectroscopy were unsuccessful. Furthermore, ^{31}P NMR spectra of mixtures of MVN (0.13–0.50 M) and NiL_a(COD) (0.025 M) in toluene-d_8 showed no evidence for the formation of an MVN complex. Thus, in the absence of HCN, complex **1** is the catalyst resting state. Kinetic studies (vide infra) suggest, however, that that a different intermediate predominates as the HCN concentration increases.

Although we have not detected any intermediates beyond complex **1** in the catalytically active hydrocyanation solutions, all of the following data implies that the catalyst comprises a single chelating ligand and one vinylarene. First, we synthesized a series of NiL(*S*) complexes [*S* = 1,5-COD, *trans*-stilbene, MVN, PhC≡CPh, L, $(CO)_2$] to test as catalyst precursors in the hydrocyanation of MVN. These complexes were prepared by ligand substitution of the zerovalent complexes $Ni(COD)_2$ and $Ni(CO)_4$, or by reduction of divalent $NiL(Br)_2$ complexes (eq 2).

$$NiL(Br)_2 + S + Zn \rightarrow NiL(S) + ZnBr_2 \qquad (2)$$

The complex NiL_a(MVN), which is proposed as a catalyst loop species, exists in solution as mixture of rapidly equilibrating diastereomers and was characterized by variable-temperature ^{31}P NMR spectroscopy (vide infra). Futher support for the identity of this complex was obtained by treatment with 1 atm of CO to generate the dicarbonyl complex $NiL_a(CO)_2$ and 1 equiv of MVN as shown by ^{31}P and ^1H NMR spectroscopy (eq 3).

$$NiL_a(MVN) + 2CO \rightarrow NiL_a(CO)_2 + MVN \qquad (3)$$

As shown in Table 5, all of the alkene and alkyne complexes were active catalysts for the asymmetric hydrocyanation of MVN and the resulting enantioselectivities depended only on the ligand L used. For example, ee's of 46% and 47% were obtained in the hydrocyanation of MVN in hexane with NiL_c(*trans*-stilbene) and NiL_c(COD), respectively (entries 12 and 13). The bis-chelate complexes $Ni(L_a)_2$ and $Ni(L_c)_2$ were either catalytically inactive (L_a, entry 5) or much less active than the mono-chelate complexes under identical conditions (L_c, entry 6 vs entry 11). The nickel dicarbonyl complexes (entries 2–4) were inactive at room temperature; however, the dicarbonyl complex $NiL_a(CO)_2$ was activated by refluxing it with MVN in toluene or heptane. Again, the ee was the same as that obtained in the other L_a catalyst systems. In this latter case, the activation process presumably occurs via dissociation of CO and the formation of small amounts of NiL_a(MVN) (eq 4) as suggested by IR and ^{31}P NMR spectroscopy.

$$NiL_a(CO)_2 + MVN \rightarrow NiL_a(MVN) + 2CO \qquad (4)$$

The addition of other vinylarenes or 2-arylpropionitriles had no significant effect on the enantioselectivity of the asymmetric hydrocyanation reaction. For example, the ee's obtained in a competitive asymmetric hydrocyanation of MVN and 4-fluorostyrene carried out in the same reaction vessel were the same as the ee's obtained for each substrate independently. Also, the enantioselectivity of the hydrocyanation of 2-vinylnaphthalene decreased only slightly (70% vs 77% ee, hexane) upon addition of optically enriched 2-(6-methoxy-2-naphthalenyl)propionitrile (89% ee, *S*). Nonlinear effects have recently been reported in a number of asymmetric catalytic reactions, however, we found no evidence of such behavior in this catalytic system.[13] For example, the enantioselectivity for MVN hydrocyanation is independent of MVN conversion, catalyst loading, and ligand to nickel ratio. Finally, we have found that the addition of up to 2.5% THF to MVN hydrocyanations with L_a in hexane also has no effect on the enantioselectivity. We therefore conclude that auxiliary ligands do not coordinate to "NiL" during any of the enantioselective steps.

The entrance into the catalytic cycle from complex **1** may occur via a small equilibrium concentration of the NiL(MVN) complex **2** (path A, Scheme 1), which we have independently prepared in the case of L_a (eq 2), and/or via the oxidative addition of HCN to generate the species NiL(H)CN, **3** (path B, Scheme 1). If the latter pathway predominates, the reaction most likely occurs with dissociation rather than hydrocyanation of COD because cyclooctenenitrile was not detected in MVN hydrocya-

(10) For a tabulation of σ values, see: March, J. Effects of Structure on Reactivity. In *Advanced Organic Chemistry: Reactions, Mechanisms, and Structure*, 4th ed.; John Wiley & Sons: New York, 1992; pp 273–292.

(11) For a review of the nickel-catalyzed hydrocyanation mechanism, see: Tolman, C. A.; McKinney, R. J.; Seidel, W. C.; Druliner, J. D.; Stevens, W. R. *Adv. Catal.* **1985**, *33*, 1–46 and references therein.

(12) Bäckvall, J. E.; Andell, O. S. *Organometallics* **1986**, *5*, 2350–2355.

(13) For a discussion of this aspect of asymmetric catalysis and leading references, see: Noyori, R.; Kitamura, M. *Angew. Chem., Int. Ed. Engl.* **1991**, *30*, 49–69.

Scheme 1. Mechanism for the Asymmetric Hydrocyanation of MVN Catalyzed by L/Ni(COD)$_2$

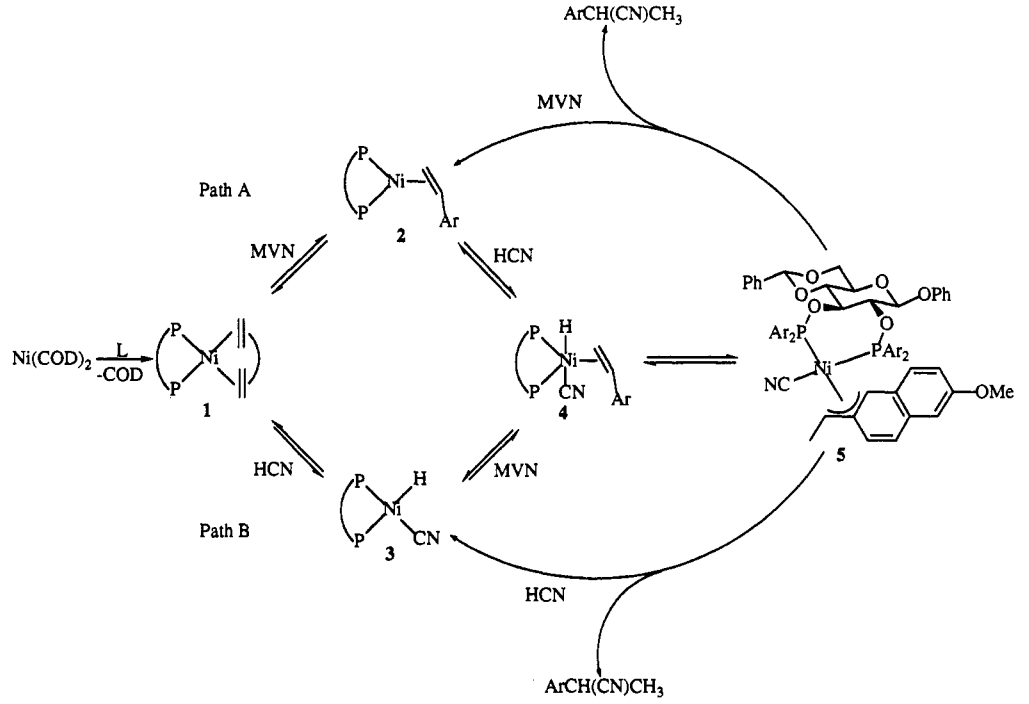

Table 5. Catalyst Precursors for the Asymmetric Hydrocyanation of MVN

entry	catalyst	ee (%)	conversion (%)
1	Ni(COD)$_2$		0
2	NiL$_a$(CO)$_2$		1[a]
3	NiL$_b$(CO)$_2$		1[a]
4	NiL$_d$(CO)$_2$		<1[a]
5	Ni(L$_a$)$_2$		0[b]
6	Ni(L$_c$)$_2$	nd	10[b]
7	NiL$_a$(COD)	77%	93[b]
8	NiL$_a$(*trans*-stilbene)	79	42[c]
9	NiL$_a$(PhC≡CPh)	74	62[c]
10	NiL$_a$(MVN)	86	52[d]
11	NiL$_c$(COD)	nd	55[b]
12	NiL$_c$(COD)	47	44[e]
13	NiL$_c$(*trans*-stilbene)	46	49[e]

[a] 0.65 mmol MVN, 0.025 mmol catalyst, 0.76 mmol HCN in 3 mL of C_6H_6 after 24 h at room temperature. [b] 0.65 mmol MVN, 0.010 mmol catalyst, 0.76 mmol HCN in 5 mL of C_6H_6 after 1 h. [c] 0.65 mmol MVN, 0.65 mmol HCN in 2 mL of C_6H_6 after 2 h. [d] 0.05 mmol MVN, 0.05 mmol HCN in 2.5 mL of hexane after 1 h. [e] 0.16 mmol MVN, 0.018 mmol catalyst, 0.16 mmol HCN in 2 mL of hexane after 16 h.

nation reaction mixtures. For comparison, in M(DIOP)[14] (M = Pt, Pd) systems, the more stable and spectroscopically detectable M(DIOP)(H)(CN) complex forms directly from M(DIOP)-(norbornene) via dissociation of norbornene (eq 5).[5b] In either

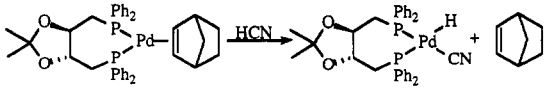

(5)

event, formation of the hydrido alkene complex NiL(MVN)-(H)CN (**4**) occurs and is followed by an insertion reaction to produce the (η^3-benzyl)nickel cyanide intermediate **5**.[15] Although this allyl-type species has not been directly detected, the exclusively branched regioselectivity observed in the asymmetric hydrocyanation reaction strongly supports its intermediacy. This regioselectivity is in sharp contrast to the preference for linear nitriles usually observed in the hydrocyanation of terminal alkenes with Ni[P(O-*o*-tolyl)$_3$]$_3$ or Ni[P(O-*p*-tolyl)$_3$]$_4$.[11] Furthermore, the hydrocyanation of 1,3-butadiene with Ni[P(O-*o*-tolyl)$_3$]$_3$ or Ni-[P(OEt)$_3$]$_4$ produces a detectable η^3-allyl species and an η^3-allyl species has also been proposed for the hydrocyanation of styrene by Ni[P(O-*o*-tolyl)$_3$]$_3$.[11,12,16] Examples of other nickel benzyl complexes exhibiting similar allylic interactions in the solution and solid state are also known.[17]

The branched nitrile is formed irreversibly in the final reductive elimination step. This conclusion is based on the independence of the enantioselectivity with reaction time or substrate conversion, and with the observation that the optical activity of enriched nitrile is unchanged when the enriched nitrile is stirred with the catalyst and HCN. Similar observations on the irreversibility of the reductive elimination step have been made for the hydrocyanation of 3-pentenenitrile, 1,3-butadiene, and 1,3-cyclohexadiene.[11,12,18]

Kinetic Studies. A preliminary analysis of the reaction kinetics of the NiL$_a$(COD) system was conducted by determining the initial rates of reaction (t = 1 min, 25 °C) while independently varying the initial HCN, MVN, and nickel concentrations. These studies were carried out by rapidly adding toluene solutions of the catalyst to toluene solutions of MVN and HCN at ambient temperature. After 1 min, aliquots of the reaction mixture were diluted into cold toluene (−78 °C), thoroughly sparged with nitrogen, and analyzed by GC.

Given the initial HCN and MVN concentrations shown in Figure 1, the initial rate is first order in nickel concentration (k_{obs} = 39 min^{-1}) over the nickel concentration range (3.4–17) × 10^{-4} M. A plot of k_{obs} vs [HCN]$_o$ shows first-order behavior at low HCN concentrations[19] (Figure 2, [HCN]$_o$ = 0.006–0.021 M, k_{HCN} = 1.4 min^{-1}) and then becomes essentially zero-order at higher HCN concentrations ([HCN]$_o$ = 0.037–0.16 M). The

(14) DIOP = *trans*-4,5-bis[(diphenylphosphino)methyl]-2,2-dimethyl-1,3-dioxolane.

(15) Our attempts to detect intermediates **4** or **5** by ^{31}P NMR spectroscopy gave ambiguous results. The addition of HCN to NiL$_a$(MVN) at low temperature caused a rapid decomposition of the reaction mixture and the formation of a complex mixture of products as determined by ^{31}P NMR spectroscopy.

(16) Tolman, C. A.; Seidel, W. C.; Druliner, J. D.; Domaille, P. J. *Organometallics* **1984**, *3*, 33–38.

(17) (a) Favero, G.; Issa, S.; Turco, A.; Vettori, U. *J. Organomet. Chem.* **1986**, *315*, 237–243. (b) Carmona, E.; Marín, J. M.; Paneque, M.; Poveda, M. L. *Organometallics* **1987**, *6*, 1757–1765. (c) Lehmkuhl, H.; Keil, T.; Benn, R.; Rufinska, A.; Krüger, C.; Poplawska, J.; Bellenbaum, M. *Chem. Ber.* **1988**, *121*, 1931–1940. (d) Carmona, E.; Paneque, M.; Poveda, M. L. *Polyhedron* **1989**, *8*, 285–291. (e) (1) Cámpora, J.; Gutiérrez, E.; Poveda, M. L.; Ruiz, C.; Carmona, E. *J. Chem. Soc., Dalton Trans.* **1992**, 1769–1774.

(18) The reductive elimination step in butadiene hydrocyanation is essentially irreversible at 25 °C, but oxidative addition of the product allylic nitriles to Ni(0) will occur at elevated temperatures.

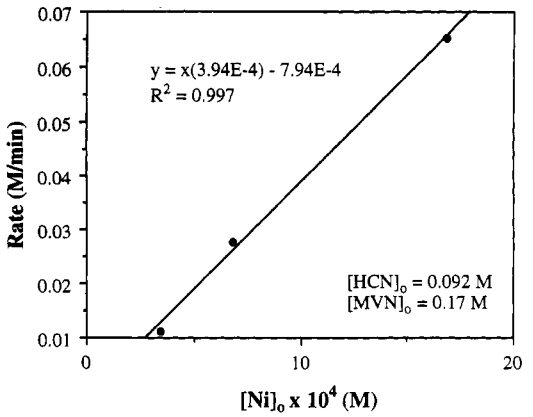

Figure 1. Initial rate of MVN hydrocyanation vs $NiL_a(COD)$ concentration.

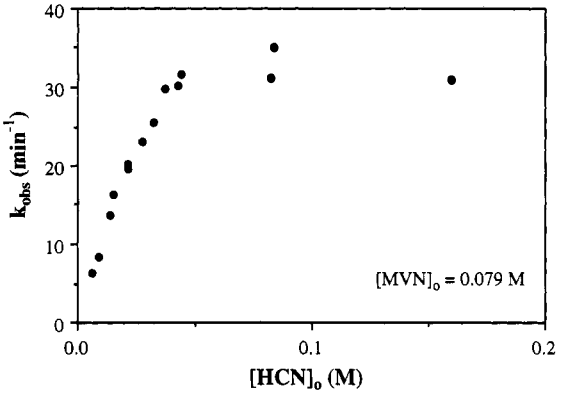

Figure 2. K_{obs} vs initial HCN concentration for $NiL_a(COD)$-catalyzed MVN hydrocyanation.

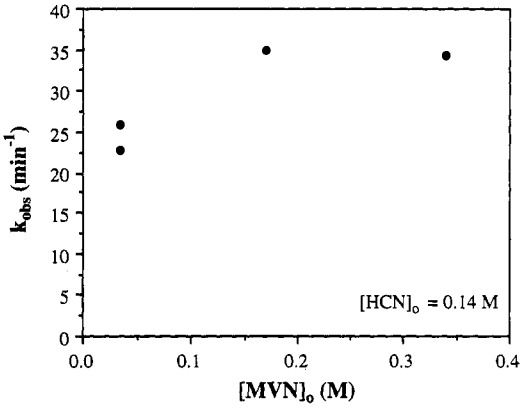

Figure 3. Initial MVN concentration vs k_{obs} for $NiL_a(COD)$-catalyzed MVN hydrocyanation.

initial rates are also essentially zero-order with respect to MVN over the concentration range [MVN]$_0$ = 0.034–0.34 M, as shown in Figure 3.[20,21]

On the basis of these results, the $NiL_a(COD)$-catalyzed hydrocyanation of MVN should follow zero-order kinetics as long as HCN and MVN saturation conditions prevail. A kinetic analysis of MVN hydrocyanation taken to 85% conversion under HCN and MVN saturation conditions (Figure 4), however, did not fit a simple zero-order model. We attribute this deviation to a concurrent, irreversible oxidation of the catalyst by HCN (eq 6). The sensitivity of zerovalent nickel phosphite complexes to

(19) Relative to [HCN]$_0$, a substantial amount of HCN is consumed in one minute at these low HCN concentrations. Thus, the measured rates at these low concentrations do not reflect the instantaneous rate at [HCN] = [HCN]$_0$. The plot actually corresponds to a plot of ([HCN]$_0$ − [HCN])/[Ni]$_0$ vs [HCN]$_0$. For a first-order reaction in [HCN] at constant [Ni]$_0$, the plot will be linear with a slope of $(1 - e^{-k})$/[Ni]$_0$ and a y intercept of zero. Details are given in the supplementary material.

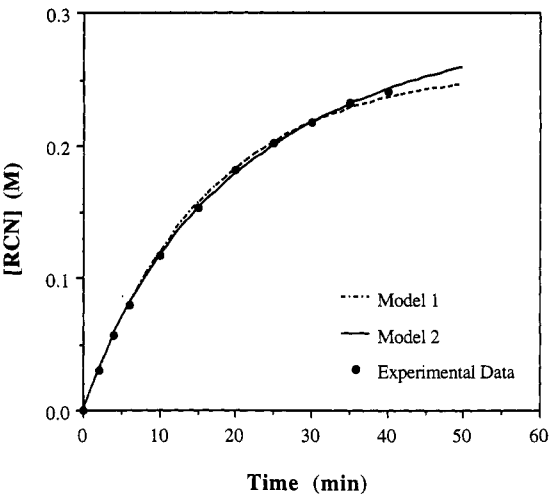

Figure 4. Calculated curves and experimental data for MVN hydrocyanation catalyzed by $NiL_a(COD)$ ([MVN]$_0$ = 0.28 M, [HCN]$_0$ = 0.42 M, [Ni]$_0$ = 5.9 × 10^{-4} M).

$$NiL_a(COD) + 2HCN \rightarrow Ni(CN)_2 + L_a + H_2 + COD \quad (6)$$

oxidation by strong acids[22,23] or HCN[11,24] has been documented, and this process accounts for the eventual deactivation of the NiL catalyst system. With this catalyst deactivation step, the data can be fit (Figure 4) to the simplified, two-step kinetic model shown below (model 1) in which the rate of nitrile formation is first order in nickel and the oxidation of the catalyst is incorporated as a process first order in both catalyst and HCN.

model 1

$$(1)\ d(RCN)/dt = [Ni]k_1 \qquad k_1 = 27\ min^{-1}$$

$$(2)\ -d[Ni]/dt = [Ni][HCN]k_2 \qquad k_2 = 0.15\ M^{-1}\ min^{-1}$$

In terms of the mechanism outlined in Scheme 1, the kinetic data implies that the catalyst resting state shifts from the NiL_a-(COD) complex to a nickel complex containing both MVN and HCN, either **4** and/or **5**, as the HCN and MVN concentrations are increased. At relatively moderate HCN and MVN concentrations the rate of formation of **4** or **5** (k_f, eq 7) becomes much

$$NiL_a(COD) + HCN + MVN \underset{k_r, +COD}{\overset{k_f, -COD}{\rightleftharpoons}} \mathbf{4}, \mathbf{5} \xrightarrow{k_p} RCN \quad (7)$$

faster than their rate of disappearance (k_r, k_p, eq 7) and essentially all of the nickel is converted to complexes **4** or **5**. Further increases in the HCN or MVN concentration do not increase the concentration of **4** or **5**, therefore the rate of nitrile formation becomes independent of the HCN and MVN concentrations.[25]

(20) For the first two data points, the MVN concentration falls to 6% ([Ni]$_0$ = 0.0014 M) and 43% ([Ni]$_0$ = 0.00073 M) of its initial value ([MVN]$_0$ = 0.035 M) in the first minute. Thus the measured rate reflects a large change in the MVN concentration and is not a true reflection of the rate at [MVN] = 0.035 M. Even so, these rates are 67% and 76% of rates observed at 10 times the initial MVN concentration.

(21) Similar HCN and MVN saturation kinetics were observed using NiL_a-(MVN) as the catalyst.

(22) Tolman, C. A. *J. Am. Chem. Soc.* **1970**, *92*, 4217–4222.

(23) Eaton, D. R.; McGlinchey, M. J.; Moffat, K. A.; Buist, R. J. *J. Am. Chem. Soc.* **1984**, *106*, 8110–8116.

(24) Tolman, C. A.; McKinney, R.; Druliner, J. D.; Casalnuovo, A. L. Unpublished results.

(25) This type of saturation kinetics is well known in enzyme catalysis; see, for example: Bell, J. E.; Bell, E. T. *Proteins and Enzymes*; Prentice-Hall: Englewood Cliffs, 1988.

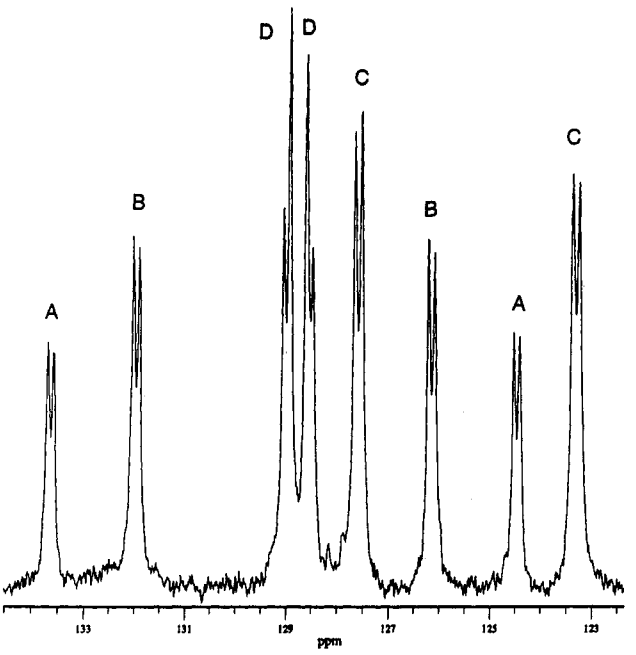

Figure 5. ^{31}P NMR spectrum of $NiL_a(MVN)$ in toluene-d_8 at −30 °C (202 MHz). Doublet pairs for the diastereomers are indicated by A–D.

Accordingly, a more complex kinetic model (model 2) derived from the mechanism in Scheme 1 also fit the data in Figure 4 well.[26]

model 2

$$1 + HCN \underset{k_{-1}}{\overset{k_1}{\rightleftarrows}} 3 \qquad k_1 = 1940\ M^{-1}\ min^{-1},\ k_{-1} = 0.005\ min^{-1}$$

$$3 + MVN \underset{k_{-2}}{\overset{k_2}{\rightleftarrows}} 5 \qquad k_2 = 921\ M^{-1}\ min^{-1},\ k_{-2} = 0.013\ min^{-1}$$

$$5 \xrightarrow{k_3} RCN + 1 \qquad k_3 = 33\ min^{-1}$$

$$5 + HCN \xrightarrow{k_4} Ni(CN)_2 \qquad k_4 = 0.21\ M^{-1}\ min^{-1}$$

By analogy to the nickel-catalyzed hydrocyanation of conjugated dienes and styrene in which the buildup of the η^3-alkyl intermediate can be directly observed,[11,12] we presume the (η^3-benzyl)nickel cyanide complex **5**, rather than **4**, is the predominant complex. We also note that no alkene hydride complexes of the type **4** have been directly observed in other hydrocyanation systems.

Enantioselectivity. If path A (Scheme 1) represents the the primary kinetic path, then the earliest point in this mechanism in which chiral recognition of MVN can occur is in the formation of the NiL(MVN) complex **2**. The ^{31}P NMR spectrum of NiL_a-(MVN), shown in Figure 5, shows the presence of four pairs of doublets in an approximately 15:23:31:31 ratio at −30 °C. We assign these resonances to the four diastereomers which result from coordination of opposite faces of MVN to the C_1 symmetric NiL_a group as shown below. Even though this ligand system gives a very high enantioselectivity for the hydrocyanation of MVN, the equilibrium distribution (vide infra) of the diastereomers found in the ^{31}P NMR spectrum of **2** shows that there is not a large ground state preference for binding either MVN enantioface. Similar results were obtained with the NiL(*trans*-stilbene) complexes (L = $L_{a,c}$). In this case, two pairs of doublets were observed in the ^{31}P NMR spectrum at 25 °C.[27] An analysis similar to that shown below shows that the coordination of NiL to the *re* and *si trans*-stilbene faces should result in two diastereomers as found in the ^{31}P NMR spectrum. Although the equilibrium distribution of the NiL(*trans*-stilbene) diastereomers is not large in either case (L_a, 2.0:1; L_c, 1.3:1), we note that the differentiation of the enantiofaces increases as the electron-withdrawing character of the *P*-aryl substituent increases.

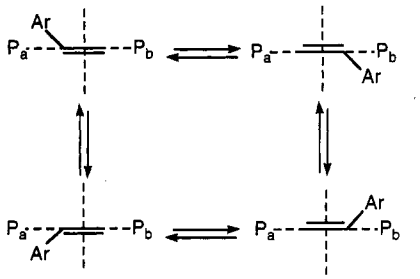

Variable-temperature ^{31}P NMR spectra of **2** show that the diastereomers are undergoing rapid exchange. The resonances broaden and coalesce into a broad singlet as the temperature is increased to 70 °C.[28] The increased line broadening that occurs upon addition of MVN to $NiL_a(MVN)$ also indicates that associative exchange occurs with uncomplexed MVN. Variable-temperature ^{31}P NMR magnetization transfer experiments show that these diastereomers interconvert with a pseudo-first-order rate constant of about $10^3\ s^{-1}$ at 25 °C in the absence of added MVN.[29] With regard to eq 8, which has been simplified to show only two diastereomers,[30] the relative rates of formation of these diastereomers of **2** (k_{R_f}, k_{S_f}) will have no effect on the overall enantioselectivity if their relative concentrations are under equilibrium control. These diastereomers will be equilibrated if

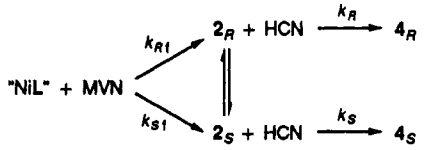

(8)

the oxidative addition of HCN to **2** is much slower than the interconversion of the diastereomers (i.e $[HCN]k_R$ and $[HCN]k_S \ll 10^3\ s^{-1}$). Although the rate of HCN oxidative addition to **2** has not been measured, the insensitivity of the enantioselectivity to the concentration of HCN ($[HCN]_o$ = 0.0088–0.16 M, $[MVN]_o$ = 0.080 M, $[Ni]_o$ = 0.00084 M) suggests that the diastereomers are under equilibrium control.[31]

If path B predominates, the initial chiral recognition of MVN occurs in the formation of **4**. The rate of interconversion between the diastereomers of **4** is unknown; however, deuterium-labeling studies show that the formation of **4** is readily reversible in the L_c and L_d systems (vide infra). *Therefore, we propose that the enantioselectivity is determined in the insertion and/or reductive elimination steps.*

(26) The set of rate constants shown in model 2 do not constitute a unique fit to the data. Provided k_1 and k_2 are large compared to k_{-1}, k_{-2}, and k_3, other suitable fits can be obtained. See supplementary material for other solutions.

(27) The exchange of uncomplexed *trans*-stilbene with complexed *trans*-stilbene in the NiL(*trans*-stilbene) complexes is not fast enough at 25 °C to affect the ^{31}P NMR line shape. However, the addition of 4,4′-dimethoxystilbene to NiL_a(*trans*-stilbene) rapidly produces a mixture of the stilbene complexes. Furthermore, the ratio of the two NiL_a(*trans*-stilbene) diastereomers is unaffected. Therefore, the ratio of diastereomers observed in the NiL(*trans*-stilbene) complexes is under thermodynamic and not kinetic control.

(28) We have been unable to observe the fast exchange limit because the compound decomposes too rapidly at temperatures > 70 °C.

(29) Complete quantitative modeling of the exchange in this complex system was unsuccessful.

(30) The *R* and *S* labeling used in eq 8 (e.g. 2_R, 2_S) denotes intermediates which lead to *R* or *S* nitriles, respectively.

(31) The hydrogen pressure dependence of the enantioselectivity in the rhodium- catalyzed asymmetric hydrogenation of acetamidoacrylates is the classic example of this type of effect; see: Landis, C. R.; Halpern, J. *J. Am. Chem. Soc.* **1987**, *109*, 1746–1754.

Table 6. Nitrile Deuterium Content from MVN-d_2 Hydrocyanation[a]

	deuterium content (%)				
ligand	d_3	d_2	d_1	d_0	conversion (%)
MVN-d_2		92.3	7.2	.5	
L_a	1	94	5	0	76
L_a[b]	2	90	8	0	87
L_b	6	87	7	0	50
L_c	31	50	15	3	69
L_d	29	50	18	3	68

[a] 0.49 mmol MVN-d_2, 0.015 mmol Ni(COD)$_2$, 0.015 mmol ligand, 0.50 mmol HCN in 5 mL of hexane. [b] 0.25 mmol MVN-d_2, 0.18 mmol Ni(COD)$_2$, 0.015 mmol L_a, 0.26 mmol HCN in 2 mL of hexane.

Deuterium Labeling. In such a multistep mechanism, knowledge of the relative rates of the individual steps is crucial to understanding the observed enantioselectivity. Information about the relative rates of formation and disappearance of the NiL(MVN)(H)CN complex **4** and the (η^3-benzyl)nickel cyanide complex **5** was obtained by hydrocyanating terminally labeled 6-methoxy-2-vinyl(2′-d_2)naphthalene (92% d_2), MVN-d_2, using catalysts prepared from Ni(COD)$_2$ and ligands L_{a-d} (eq 9).

$$\mathrm{ArCH{=}CD_2 + HCN \rightarrow ArCH(CN)(CD_xH_{3-x})} \quad (9)$$

Product nitriles were isolated and characterized by ^{1}H, ^{2}H and ^{13}C{^{1}H} NMR spectroscopy. In all cases, deuterium was incorporated exclusively in the β-methyl position (≥98%). The relative amounts of deuterium isotopomers, corresponding to the degree of deuterium incorporation in the β-methyl group (see Table 6), were determined by integration of the benzylic carbon resonances in the ^{13}C{^{1}H} NMR spectra. These resolved singlet resonances are shifted upfield 0.074 ± 0.002 ppm for each deuterium present on the adjacent methyl carbon.[32]

The most striking result of this study is that the extent of deuterium scrambling decreases with the electron-withdrawing character of the *P*-aryl substituent, decreasing in the order $L_d \approx L_c \gg L_b > L_a$, as shown in Table 6.[33] In fact, only a trace of deuterium scrambling was observed when the strongly electron-withdrawing trifluoromethyl derivative L_a was used. As shown in Scheme 2, H/D exchange can occur from complex **4** via insertion of MVN-d_2 into the Ni–H bond to form complex **5**, rotation of the β-methyl group, β-deuteride elimination from **5** to form NiL(MVN-d_1)(D)CN (**4′**), followed by exchange of complexed MVN-d_1 and/or DCN with uncomplexed MVN-d_2 or HCN. The extent of deuterium scrambling observed for the NiL$_c$(COD) and NiL$_d$(COD) catalysts indicates that the formation of both complexes **4** and **5** (Scheme 1) is readily reversible for the more electron-donating ligand systems.[34] The relative lack of exchange observed for the L_a and L_b systems must result from a nearly irreversible formation of complex **4** and/or **5**. For the mechanism shown below in eq 10, if $k_{-1} \gg k_2$, then the degree of scrambling will depend on the ratio k_3/k_{-2}. That is, the barrier to reductive elimination from the (η^3-benzyl)nickel cyanide complex **5** (k_3, eq 10) decreases relative to the barrier to β-hydride elimination (k_{-2}) as the *P*-aryl substituent becomes more electron withdrawing. In the limit of this behavior, $k_3 \gg k_{-2}$, β-hydride elimination cannot compete with reductive elimination, therefore, the insertion reaction becomes irreversible. Alternatively, if $k_2 \gg k_{-1}$, then the degree of scrambling will depend on the relative rates for reductive elimination vs MVN/HCN exchange (i.e. [**5**]k_3 vs [**4**]k_{-1}). We therefore propose that the primary effect

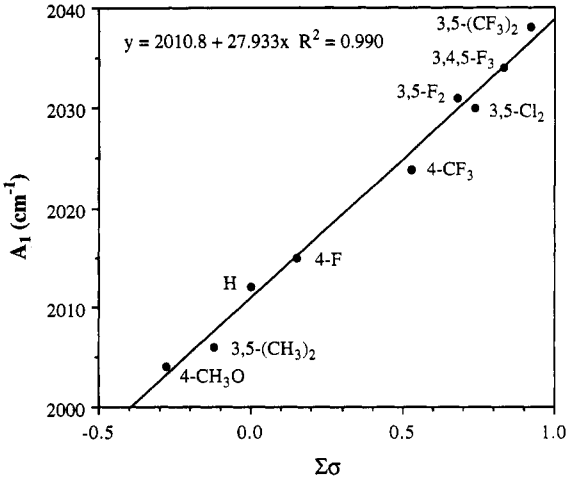

Figure 6. Correlation of σ_m and σ_p with the A_1 stretching frequency in NiL(CO)$_2$ complexes.

brought about by the more electron-withdrawing ligand substituents is an increase in the value of k_3, although other parts of the mechanism are probably also affected.[35] This explanation satisfies both kinetic scenarios and is consistent with studies which suggest that less basic phosphorus ligands (i.e. more electron deficient) accelerate the rate of reductive elimination reactions.[2f-k]

$$\mathbf{2}\text{ or }\mathbf{3} \underset{k_{-1}}{\overset{k_1}{\rightleftarrows}} \underset{\mathbf{4}}{\mathrm{NiL(MVN)(H)CN}} \underset{k_{-2}}{\overset{k_2}{\rightleftarrows}} \underset{\mathbf{5}}{\mathrm{NiL(CN)(\eta^3\text{-benzyl})}} \xrightarrow{k_3} \text{nitrile} + \mathrm{NiL} \quad (10)$$

The effect of the *P*-aryl substituents on the overall ligand basicity is clearly seen from an analysis of the IR spectra of the nickel dicarbonyl derivatives, Ni(CO)$_2$L. The electronic properties of phosphorus ligands have often been correlated with CO stretching frequencies in metal carbonyls.[2b,36,37] For example, Tolman has shown that the A_1 carbonyl stretching frequency in Ni(PR$_3$)(CO)$_3$ complexes can be calculated from empirically derived substituent parameters.[37] In that study, the effects of *meta* and *para* *P*-aryl substituents on the A_1 stretching frequency were small, but consistent with the electronic character of the substituent.[38] Table 3 shows the carbonyl stretching frequencies for a variety of *ortho*-, *meta*-, and *para*-substituted Ni(CO)$_2$L complexes as well as the ee's obtained in MVN hydrocyanations using these ligands with Ni(COD)$_2$. The effect of the aryl substituent is strongly manifested in the A_1 stretching frequency which increases 34 cm^{-1} from the electron-donating 4-methoxy group to the electron-withdrawing 3,5-bis(trifluoromethyl) group. In fact, the A_1 frequency correlates linearly with $\Sigma\sigma_m$ and σ_p values as shown in Figure 6. Similar plots between log(S/R) and $\Sigma\sigma$ or log(S/R) and the carbonyl stretching frequency were not strictly linear. In this regard, Jacobsen has reported linear correlations between σ_p and log(S/R) for an asymmetric

(32) The integration of β-carbon resonances for the analysis of deuterium labeling experiments in Rh-catalyzed hydrocarbonylation experiments has recently been reported. MacDougall, J. K.; Simpson, M. C.; Cole-Hamilton, D. J. *J. Chem. Soc., Dalton Trans.*, in press.

(33) The same trend was observed using DCN in the hydrocyanation of MVN with NiL$_a$(COD) and NiL$_c$(COD).

(34) For simplicity, this analysis treats the deuterium scrambling experiments in terms of the behavior of a single diastereomer. The total scrambling observed will of course depend on the additive effects of all of the diastereomeric pathways.

(35) For supporting studies on the effect of ligand basicity and reductive elimination see ref 2f–k. We have proposed the simplest explanation for the H/D exchange data. The ground state energies of the intermediates and the barriers for the other fundamental steps can be affected by changes in the electronic properties of the ligand. Several convincing studies have shown that oxidative addition reactions of Ir(I) are accelerated by more electron-donating ligands. Other studies suggest that activation barriers for insertion of alkenes into metal hydride bonds are lowered by more electron-donating ligands. See ref 2a–g and 2m.

(36) Jolly, P. W. Lewis-base Nickel Carbonyl Complexes. In *Comprehensive Organometallic Chemistry: The Synthesis, Reactions and Structure of Organometallic Compounds*; Wilkinson, G., Ed.; Pergamon: Oxford, 1982; Vol. 6, pp 28–30.

(37) Tolman, C. A. *J. Am. Chem. Soc.* **1970**, *92*, 2953–2956.

(38) An increase of about 8 cm^{-1} in A_1 was observed in changing from P(p-C$_6$H$_4$OCH$_3$)$_3$ to P(m-C$_6$H$_4$F)$_3$. The larger changes in A_1 for the NiL(CO)$_2$ complexes are undoubtedly a reflection of the greater number of aryl substituents and phosphorus atoms.

Scheme 2. Mechanism for H/D Exchange in the Asymmetric Hydrocyanation of MVN

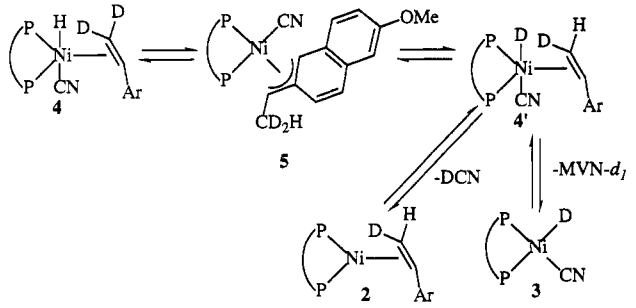

manganese-catalyzed alkene epoxidation reaction.[3a] Our analysis of the asymmetric hydrocyanation system suggests that the overall rate law changes as the ligand substituents are varied; therefore the lack of a strictly linear correlation between $\log(S/R)$ and σ, or $\log(S/R)$ and stretching frequency is not surprising.[39] In any event, the trend toward higher ee with decreasing ligand basicity is pronounced and is consistent with the decreased deuterium scrambling and an enhanced rate of reductive elimination.

The formation of the (η^3-benzyl)nickel cyanide complex **5** appears to become irreversible in the case of $\mathbf{L_a}$, however, a large normal isotope effect in the β-deuteuride elimination step (**5** → **4'**, Scheme 2) would decrease the apparent rate of β-hydride elimination relative to reductive elimination.[40] To preclude this possibility, we also examined the addition of DCN (~87% d) to an excess of MVN catalyzed by $\mathrm{NiL_a}$(PhC≡CPh). This catalyst was used instead of $\mathrm{NiL_a}$(COD) to eliminate the possibility of H/D exchange with COD protons via an insertion–elimination mechanism. In contrast to the previous experiment, H/D exchange occurs when a *hydrogen* eliminates from the (η^3-benzyl)-nickel cyanide complex **5**. The reaction was driven to 57% conversion with essentially complete consumption of DCN. The ee of the product nitrile was unaffected by the use of DCN[41] and, again, deuterium was incorporated only in the β-methyl position of the nitrile and in the terminal carbon of the alkene (both cis and trans isomers). The isolated alkene comprised 90% d_0 and 10% d_1, whereas the isolated nitrile comprised 22% d_0, 75% d_1, and 3% d_2 as opposed to the expected values of 13% d_0 and 87% d_1 for an irreversible insertion reaction. We conclude that k_3 does increase markedly for ligands with electron-withdrawing substituents, but that the formation of the (η^3-benzyl)nickel cyanide complex **5** is not strictly irreversible for $\mathbf{L_a}$.[42]

Another interesting electronic effect in this hydrocyanation system involves the effect of the substrate *para* substituent. In this case, electron-donating substiutents generally lead to higher ee's. To probe this facet of the reaction mechanism, terminally labeled 4-trifluoromethylstyrene-d_2 (89% d_2) and 4-methylstyrene-d_2 (92% d_2) were hydrocyanated (58% and 85% conversion, respectively) with $\mathbf{L_a}$ in a fashion similar to the hydrocyanation of MVN-d_2. As before, the ee's of the isolated nitriles were unaffected by deuterium substitution and deuterium was incorporated exclusively in the β-methyl position (≥98%). Integration of the $^{13}C\{^1H\}$ NMR spectra of the product nitriles showed 13% d_1, 61% d_2, 26% d_3 for 2-[4-(trifluoromethyl)phenyl]propionitrile and 12% d_1, 77% d_2, 11% d_3 for 2-(4-methylphenyl)propionitrile. Thus, in contrast to the ligand substituents, H/D exchange decreases as the electron-donating character of the substrate substituent increases. This apparent paradox can still be interpreted in terms of an increase in k_3, because other studies suggest that, unlike ligand substituents, the rate of reductive elimination increases with an increase in the σ/π donor strength of the eliminating alkyl group.[43]

The reasons for the pronounced solvent effects are unclear. Unlike the ligand and substrate electronic effects, the decrease in ee observed in polar solvents appears unrelated to the k_3/k_{-2} ratio. We have found that the extent of deuterium scrambling in the $\mathrm{NiL_a}$(COD)-catalyzed hydrocyanation of MVN-d_2 in acetonitrile (27% ee) or THF (65% ee) was not significantly different than in hexane. The solvent effect may indicate that charge separation is an important component in some of the intermediates or transition states but a more definitive explanation will require a better understanding of the reacton mechanism.

Electronic Effect and Enantioselectivity. The detailed reasons for the correlation between higher enantioselectivities and electron-withdrawing aryl substituents must remain speculative because the relative rates of many of the fundamental steps and the structures of the intermediates are still largely unknown. The experimental evidence for the NiL system clearly shows that the enantioselectivity is not controlled by direct steric interactions between the *meta* or *para* *P*-aryl substituents and the alkene substrate. This is further supported by chemical models of prototypical NiL complexes and solid state structures of L complexes.[44] In similar chiral, bidentate ligand systems, other workers have stressed the importance of the conformational positions of the *P*-aryls (i.e. axial vs equatorial) in creating the chiral pocket of the catalyst.[45] Although such steric factors are probably important, our data shows that there is also a strong electronic component present in the NiL catalyst system that can be used to increase the *inherent preference* for *S*- vs *R*-nitriles. We suggest that the barrier for reductive elimination of nitrile from **5** decreases disproportionately for one of the *S* pathways as the electron density at nickel is decreased and that this is the origin of the electronic effect. A better understanding of this possibility will depend on a detailed description of the various structures of **5** and the transition states leading to reductive elimination. In principle, such electronic effects should have wider applications in other organometallic processes. We have recently shown that electron-*donating* aryl substituents on related phosphinite systems dramatically enhances the enantioselectivity of the Rh-catalyzed asymmetric hydrogenation of acetamido acrylates.[4c] It is interesting to note that in this instance an oxidative addition of H_2 to a Rh complex is involved in a key enantioselective step[31] and the electron density at Rh has been linked to the enantioselectivity of the asymmetric hydrogenation reaction.[46]

Although ground state arguments can be misleading in the analysis of asymmetric catalytic systems,[31] we are also intrigued by the observation that a greater differentiation between enantiotopic faces of *trans*-stilbene occurs for $\mathrm{NiL_a}$(*trans*-stilbene)

(39) Under HCN and MVN saturation conditions, the rate law for the mechanism in equation 10 is given by $R = ([\mathrm{Ni}]_o k_2 k_3)/(k_2 + k_{-2} + k_3)$ where $[\mathrm{Ni}]_o = [\mathbf{4}] + [\mathbf{5}]$ and $d[\mathbf{5}]/dt = 0$. Thus the form of the rate law will be very sensitive to the relative magnitudes of the individual rate constants.

(40) We assume a neglible secondary isotope effect on the reductive elimination.

(41) In principle, the magnitudes of isotope effects for the diastereotopic *R* and *S* pathways can differ, and this can lead to a change in the observed ee.

(42) The mechanistic changes brought about by the ligand substituents are similar to the changes observed in the hydrocyanation of conjugated dienes vis á vis isolated alkenes. For example, the insertion reactions of 1,3-butadiene with $\mathrm{HNi((P(O\text{-}o\text{-}tolyl)_3)_3(CN)}$ and 1,3-cyclohexadiene with $\mathrm{Ni(P(OPh)_3)_4}$/HCN are irreversible, whereas insertion reactions with isolated alkenes such as ethylene and 3-pentenenitrile are readily reversible. See refs 11 and 12.

(43) For supporting studies on the effect of substrate donor strength on reductive elimination see ref 2f,g,k. Other studies suggest that the barrier to insertion of an alkene into a metal–hydride or metal–alkyl bond is decreased with increasing donor strength of the substrate. See ref 2m and 17c.

(44) The solid-state structures of two Rh(I) complexes incorporating $\mathbf{L_a}$ and $\mathbf{L_d}$ and two Rh(I) complexes containing ligand analogues derived from 1,2-cyclohexanediol have been solved by single-crystal X-ray diffraction. Chemical models of prototypical nickel complexes have also been constructed using CAChe software (MM2).

(45) (a) Knowles, W. S. *Acc. Chem. Res.* **1983**, *16*, 106–112. (b) Oliver, J. D.; Riley, D. P. *Organometallics* **1983**, *2*, 1032–1038. (c) Brown, J. M.; Evans, P. L. *Tetrahedron* **1988**, *44*, 4905–4916. (d) Pavlov, V. A.; Klabunovskii, E. I.; Struchkov, Y. T.; Voloboev, A. A.; Yanovsky, A. I. *J. Mol. Catal.* **1988**, *44*, 217–243. (e) Bogdan, P. L.; Irwin, J. J.; Bosnich, B. *Organometallics* **1989**, *8*, 1450–1453. (f) Seebach, D.; Plattner, D. A.; Beck, A. K.; Wang, Y. M.; Hunziker, D. *Helv. Chim. Acta.* **1992**, *75*, 2171–2209.

(46) Bender, B. R.; Koller, M.; Nanz, D.; von Philipsborn, W. *J. Am. Chem. Soc.* **1993**, *115*, 5889–5890.

(2.0:1) than for NiL_c(*trans*-stilbene) (1.3:1). The greater ground state differentiation for the L_a system ($\Delta\Delta G \approx 0.4$ kcal/mol) may arise from a shortening of Ni–P bond lengths which should, in turn, magnify ligand–substrate interactions. Further work is needed to document such ground state effects and to establish how transition states are affected.

Laboratory Preparations of the Nitriles with L_a. The utility of any asymmetric hydrocyanation catalyst depends not only on the enantioselectivities obtained but also on the catalytic turnover ($mole_{RCN}/mole_{Ni}$) and rate. Although kinetic analyses have not been carried out except in the L_a/MVN system, most reactions are complete after several hours at room temperature with 1–3 mol % of the NiL_a catalyst. As shown by the previous analysis of the L_a/MVN system (vide supra), the MVN hydrocyanation rate reaches a maximum activity of about 2000 turnovers/h at room temperature. The total number of turnovers for the L_a-derived catalyst vary depending on the vinylarene substrate and the method of HCN addition, but are certainly practical for laboratory preparations. A slow addition of HCN is usually preferred in nickel-catalyzed hydrocyanation reactions because a low steady state HCN concentration minimizes oxidation of the catalyst. For example, semibatch hydrocyanations (i.e. slow, dropwise addition of HCN) of 4-chlorostyrene, 4-fluorostyrene, and MVN gave 53, 94, and 769 turnovers, respectively.[47] By comparison, a batch hydrocyanation of 4-fluorostyrene gave 61 turnovers before the catalyst deactivated.[48] MVN is an exceptional substrate in this respect because the catalytic turnover was unaffected in an analogous batch hydrocyanation (757 turnovers).[49]

From an economic standpoint, the ligand L_a is a more valuable component of the catalyst than the nickel. A consideration of the catalyst deactivation mechanism affords a simple procedure for increasing the *ligand* utility. As shown in eq 6, the catalyst deactivation occurs with HCN oxidation of the nickel center and dissociation of the *free* ligand. This latter observation is important because it suggests that the deactivated catalyst can be reactivated by adding more $Ni(COD)_2$ to the reaction mixture. In fact, using this procedure we have achieved 4400 turnovers *per ligand* (L_a) for MVN hydrocyanation *without loss of enantioselectivity*.

The extremely high regioselectivity of the $Ni(COD)_2/L_a$ catalyst coupled with the relatively high rates and turnovers make it an ideal catalyst system for preparative hydrocyanations of vinylarenes, although enantioselectivities vary considerably with the vinylarene. Thus, 2-(6-methoxy-2-naphthyl)propiopnitrile[50] and 2-(4-isobutylphenyl)propionitrile, precursors to naproxen and ibuprofen, were prepared in 96% and 77% isolated yields (conversion > 99.5% in both cases), on 5 and 1 g scales using 0.01 and 0.02 equivalents of the catalyst, respectively. Yield losses due to polymerization of these two substrates were not observed. In fact, upon careful examination, the only byproduct detected in the MVN hydrocyanation was a trace amount of 6-methoxy-2-napthyl methyl ketone which arises from the presence of adventitious oxygen.[51]

Summary and Conclusions

Diarylphosphinites derived from glucose, **L**, are excellent ligands for the Ni(0)-catalyzed asymmetric hydrocyanation of vinylarenes. The enantioselectivity of the hydrocyanation increases dramatically when the ligands contain electron-withdrawing *P*-aryl substituents. The mechanism of the reaction with MVN has been analyzed in terms of an initial HCN oxidative addition or vinylarene coordination to "NiL", followed by insertion to form an (η^3-benzyl)nickel cyanide complex, and irreversible reductive elimination of the nitrile. Kinetic studies of the NiL_a(COD) catalyzed hydrocyanation of MVN show that as the HCN concentration is increased the catalyst resting state shifts from NiL_a(COD) to a complex containing both HCN and MVN—presumably the (η^3-benzyl)nickel cyanide complex. ^{31}P NMR analysis of the postulated intermediate NiL_a(MVN) indicates very little ground state differentiation of the *re* and *si* faces of MVN and that the diastereomers are most likely equilibrated during the hydrocyanation. IR and deuterium labeling studies suggest that the primary effect of the electron-withdrawing *P*-aryl substituents is to decrease the electron-density at nickel and thereby increase the rate of reductive elimination of the product nitrile from the (η^3-benzyl)nickel cyanide complex. We propose that the enantioselectivity increases because the rate of reductive elimination from one of the (η^3-benzyl)nickel cyanide diastereomers is disproportionately increased.

In this exercise of semiempirical ligand design, we have only optimized the enantioselectivity for one reaction. We have shown that by electronic tuning of ligands from a readily available sugar one can produce a key 2-arylpropionitrile in excellent enantioselectivity and chemical yield using as little as 0.001 equiv of a Ni(0) catalyst. Our studies clearly demonstrate that even a moderate recognition afforded by a suitably chosen chiral catalyst system can be parlayed into high overall enantioselectivity by manipulating the relative rates of key steps involved in the product formation. In fact, the lessons learned here have been succesfully applied to the asymmetric hydrogenation reaction as well.[4c] Further studies on the applications of these ligand systems for other asymmetric reactions are in progress.

Experimental Section

General Methods. All reactions were carried out under a nitrogen atmosphere by using either Schlenk techniques or a Vacuum Atmospheres drybox. Solvents were distilled and degassed before use. Conversions were determined by GC using a cross-linked methylsilicone capillary column (30 m × 0.530 m). Flash column chromatography was carried out on 230–400 mesh silica (EM Reagents).[52] NMR spectra were obtained on C_6D_6 solutions using QE 300 MHz, GE Omega 500 MHz, and Nicollet 300 MHz NMR spectrometers unless stated otherwise. IR spectra were recorded of benzene solutions on a Perkin-Elmer 983G spectrophotometer. Magnetizaton transfer experiments were conducted by selective inversion of the various ^{31}P resonances (202 MHz). Enantiomeric excesses were determined by HPLC using either a Daicel Chiralcel OJ or OB column and eluting with hexane/i-PrOH mixtures as detailed below (T = 40 °C). Samples for HPLC were passed through a short pad of silica gel and eluted with 90/10 hexane/Et_2O prior to analysis. Authentic samples of the *S* nitriles were prepared from naproxen and ibuprofen as described below and were used to verify the absolute configuration of the asymmetric hydrocyanation products. Racemic mixtures of all of the nitriles were synthesized by $Ni[P(O\text{-}p\text{-}tolyl)_3]_4$-catalyzed hydrocyanation of the alkenes [8a] to verify HPLC assignments. Nickel powder, $Ni(COD)_2$, $Ni(CO)_4$, and all of the vinylarenes except 6-methoxy-2-vinylnaphthalene,[8a] 1-vinylnaphthalene, 4-phenyl-3-fluorostyrene,[53] 4-isobutylstyrene,[8a] 4-(2-methylpropenyl)styrene, and 4-(trifluoromethyl)styrene were obtained from commercial sources. Hydrogen cyanide was obtained in small cylinders from Fumico, Inc. (Amarillo, TX).

Caution! HCN is a highly toxic, volatile liquid (bp 27 °C) that is also susceptible to explosive polymerization in the presence of base catalysts. It should be handled only in a well-ventilated fume hood or drybox. Sensible precautions include not working alone and having available proper first aid equipment, HCN monitors, and Scott Air Packs. HCN should be handled by teams of at least two technically qualified individuals who have recieved appropriate medical training for treating HCN poisoning

(47) Reaction conditions: 0.40 M chlorostyrene + 0.0040 M catalyst in hexane/toluene (80/20); 0.25 M fluorostryene + 0.0025 M catalyst in toluene; 0.36 M MVN + 0.00036 M catalyst in toluene.

(48) Reaction conditions: 0.25 M fluorostyrene + 0.25 M catalyst + 0.50 M HCN in toluene.

(49) Reaction conditions: 0.33 M MVN + 0.00033 M catalyst + 0.75 M HCN in toluene.

(50) This nitrile is enriched to 93% ee upon precipitation from the bulk solution (85% ee). Further recrystallization gives the optically pure nitrile. See the experimental section.

(51) Our studies suggests that zerovalent nickel stoichiometrically oxidizes the product nitrile to the ketone in the presence of oxygen, possibly via the cyanohydrin. Thus yield losses to the ketone are very small and can be avoided by rigorous exclusion of oxygen or the use of low nickel loadings.

(52) Still, W. C.; Kahn, M.; Mitra, A. J. *J. Org. Chem.* **1978**, *43*, 2923–2925.

(53) Stille, J. K.; Su, H.; Brechot, P.; Parrinello, G.; Hegedus, L. S. *Organometallics* **1991**, *10*, 1183–1189.

(for details see: *Prudent Practices for Handling Hazardous Chemicals in Laboratories*; National Academy Press: Washington, DC, 1981; pp 45–47). Commercial HCN is stabilized with small amounts of strong acids such as H_2SO_4. Small amounts of uninhibited HCN may be obtained by vacuum transfer through Drierite. Uninhibited HCN should be stored cold. Excess HCN may be disposed of by burning or in the case of small amounts of HCN by adding to aqueous sodium hypochlorite (which converts it to the cyanate).

Preparation of Ligands. The preparation of certain O-substituted pyranose phosphinites, including the simple phenyl derivative $\mathbf{L_c}$, has been described elsewhere.[54] In general, pyranoside derivatives containing unprotected hydroxyl groups are treated with a R_2PCl reagent in the presence of a base, such as pyridine or triethylamine, to produce the desired phosphinite. Some R_2PCl reagents are commercially available, such as Ph_2PCl. R_2PCl reagents, where R = aryl or alkyl, can also be prepared in two steps by treatment of readily available dialkyl phosphites, such as dibutyl phosphite, $(BuO)_2P(O)H$, with RMgBr followed by treatment of the resulting $R_2P(O)H$ product with PCl_3.[55] Alternatively, R_2PCl reagents can be prepared by treating $(Et_2N)PCl_2$ with 2 equiv of RMgBr followed by treatment of the resulting $(Et_2N)PR_2$ product with HCl.[2n]

Bis[3,5-bis(trifluoromethyl)phenyl]chlorophosphine. 1. From $(Et_2N)PCl_2$. A 1.0 M solution of [3,5-bis(trifluoromethyl)phenyl]magnesium bromide was prepared by slow addition of 18.5 g (60 mmol) of 3,5-bis(trifluoromethyl)bromobenzene in 40 mL of THF to a slurry of Mg turnings in 20 mL of THF. After 1 h, this solution was added slowly to a solution of 5.0 g (29 mmol) of $(Et_2N)PCl_2$ in 30 mL of THF at 0 °C. After 2 h, the mixture was concentrated in vacuo. Cyclohexane (100 mL) was added and the mixture was filtered through celite to provide a solution of bis[3,5-bis(trifluoromethyl)phenyl](diethylamino)phosphine. Dry HCl was passed through this solution for 1 h. After filtration under a nitrogen atmosphere (in some instances, it was necessary to degas the solution to precipitate the amine hydrochloride) and concentration, 12.4 g (88%) of the chlorophosphine was collected as a white solid.

2. From $(BuO)_2P(O)H$. A solution of dibutyl phosphite, $(BuO)_2P(O)H$ (0.025 mol, 4.855 g), in 5 mL of Et_2O was added dropwise by an addition funnel to a slurry of KH (0.0275 mol, 1.103 g) in 10 mL of Et_2O (**caution:** H_2 evolution occurs) and stirred for 5 h at room temperature. The reaction mixture was filtered to remove excess KH (Care!!) and the resulting filtrate was treated dropwise with a solution of $(3,5\text{-}(CF_3)_2C_6H_3)MgBr$ (0.050 mol) in 15 mL of Et_2O. After 4 h, 50% aqueous Na_2HPO_4 was added, the mixture was filtered and rinsed with Et_2O. The organic layer was dried (Na_2SO_4) and concentrated. After refluxing the resulting dark solids briefly in benzene, the mother liquor was filtered to remove dark solids. Concentration of the filtrate gave 8.72 g (74%) of $(3,5\text{-}(CF_3)_2C_6H_3)_2P(O)H$. Alternatively, the product may be chromatographed on silica gel using 40% ethyl acetate in hexane as eluent. $^{31}P\{^1H\}$ NMR: δ 12.1 ppm (s, J_{PH} = 506 Hz, ^1H coupled spectrum). ^1H NMR: δ 7.27 (d, 509 Hz, 1H), 7.56 (s, 2H), 7.78 (d, 13.0 Hz, 4H).

PCl_3 (3.49 g, 0.0255 mol) was added dropwise to a solution of $(3,5\text{-}(CF_3)_2C_6H_3)_2P(O)H$ (8.72 g, 0.018 mol) in 35 mL of CH_2Cl_2. After 1.5 h, the reaction mixture was concentrated to an oil under high vacuum. The crude product was vacuum transferred under high vacuum (5 mTorr) by heating with a heat gun. The yield was 6.36 g (72%) of a white solid of about 95 mol % purity by ^{31}P and ^1H NMR spectroscopy. $^{31}P\{^1H\}$ NMR: δ 70.4 (s). ^1H NMR: 7.54 (s, 2H), 7.66 (d, J = 6.5 Hz, 4H).

Bis(4-methoxyphenyl)chlorophosphine. ^{31}P NMR: δ 85.4. ^1H NMR: δ 7.54 (m, 4H), 6.65 (m, 4H), 3.17 (s, 6H). ^{13}C NMR: δ 162.9 (s), 134.0 (d, J_{PC} = 26 Hz), 114.6 (d, J_{PC} = 8 Hz), 54.8 (s).

Bis(3,5-dimethylphenyl)chlorophosphine. ^{31}P NMR: δ 85.3. ^1H NMR: δ 7.25 (m, 4H), 6.62 (s, 2H), 1.85 (m, 12H).

Bis(3,5-difluorophenyl)chlorophosphine. ^{31}P NMR: δ 75.3. ^1H NMR δ 6.93 (m, 4H), 6.43 (m, 2H).

Bis(3,4,5-trifluorophenyl)chlorophosphine. ^{31}P NMR: δ 75.4. ^1H NMR: δ 6.59 (m).

Bis(3,5-dichlorophenyl)chlorophosphine. ^{31}P NMR: δ 74.0. ^1H NMR: δ 6.79 (t, J = 2 Hz, 2H), 7.07 (dd, 2, 7 Hz, 4H).

Bis[3,5-bis(trimethylsilyl)phenyl]chlorophosphine. ^{31}P NMR: δ 84.4. ^1H NMR: δ 0.10 (s, 36H), 7.81 (m, 2H), 8.05 (dd, J = 1.1, 8.0 Hz, 4H).

Bis(4-fluorophenyl)chlorophosphine. ^{31}P NMR: δ 80.6. ^1H NMR: δ 7.12 (m, 4H), 6.58 (m, 4H).

Bis[4-(trifluoromethyl)phenyl]chlorophosphine. ^{31}P NMR: δ 76.3. ^1H NMR: δ 7.33 (m, 8H).

Bis(2-methylphenyl)chlorophosphine. ^{31}P NMR: δ 74.2. ^1H NMR: δ 7.75 (m, 2H), 7.15 (m, 4H), 6.98 (m, 2H), 2.44 (d, 6H, J_{PH} = 3 Hz).

Bis(2,5-dimethylphenyl)chlorophosphine. ^{31}P NMR: δ 75.0. ^1H NMR: δ 7.54 (m, 2H), 6.80 (m, 4H), 2.31 (d, 6H, J_{PH} = 3 Hz), 1.92, (s, 6H).

Preparation of Phenyl 2,3-Bis-*O*-[bis[3,5-bis(trifluoromethyl)phenyl]-phosphino]-4,6-*O*-benzylidene-β-D-glucopyranoside, $\mathbf{L_a}$. A solution of $(3,5\text{-}(CF_3)_2C_6H_3)_2PCl$ (1.246 g, 2.53 mmol) in 5 mL of CH_2Cl_2 was cooled to 0 °C and added dropwise to a solution of phenyl 4,6-*O*-benzylidene-β-D-glucopyranoside (0.397 g, 1.15 mmol) and DMAP (0.030 g, 0.25 mmol) in 15 mL of CH_2Cl_2/pyridine (1:1) at 0 °C. The reaction mixture was warmed to room temperature, stirred overnight, and concentrated to dryness in vacuo. The resulting solids were slurried in hot benzene and filtered, and the filtrate concentrated in vacuo to a dry white solid. These white solids were washed with about 2 mL of cold hexane and dried in vacuo to give 1.135 g (79%) of $\mathbf{L_a}$. $^{31}P\{^1H\}$ NMR: δ 108.4 (s, 1P), 107.5 (s, 1P). ^1H NMR: δ 2.98 (m, 1H), 3.15 (t, J = 9.2 Hz, 1H), 3.27 (t, 10.2 Hz, 1H), 3.88 (dd, 4.9, 10.4 Hz, 1H), 4.19 (m, 2H), 4.69 (m, 1H), 4.94 (s, 1H), 6.33 (d, 7.9 Hz, 2H), 6.69 (t, 7.3 Hz, 1H), 6.88 (t, 8.0 Hz, 2H), 6.97 (m, 2H), 7.05 (m, 3 H), 7.35 (s, 2H), 7.39 (s, 2H), 7.82 (m, 8H). Anal. C, H, P.

Preparation of Phenyl 2,3-Bis-*O*-[bis(3,5-dimethylphenyl)phosphino]-4,6-*O*-benzylidene-βf-D-glucopyranoside, $\mathbf{L_d}$. A solution of $(3,5\text{-}(CH_3)_2C_6H_3)_2PCl$ (0.582 g, 2.1 mmol) in 2 mL of CH_2Cl_2 was cooled to 0 °C and added dropwise to a solution of DMAP (0.013 g, 0.11 mmol) and phenyl 4,6-*O*-benzylidene-β-D-glucopyranoside (0.345 g, 1.0 mmol) in a mixture of 2 mL pyridine and 2 mL CH_2Cl_2 at 0 °C. The reaction mixture was warmed to room temperature and stirred overnight. Et_2O/hexane (1:1, 10 mL) was added to the reaction mixture, and the resulting solids were removed by filtration (2 mL hexane rinse). The filtrate was concentrated in vacuo to give 0.796 g (96%) of $\mathbf{L_d}$ as a white solid. ^{31}P NMR: δ 117.5 (d, J_{P-P} = 2 Hz, 1P) 123.0 (d, 2 Hz, 1P). ^1H NMR: δ 1.81 (s, 6H), 1.88 (s, 6H), 1.96 (s, 6H), 1.97 (s, 6H), 3.09 (td, 5.0, 9.6 Hz, 1H), 3.24 (t, 10.1 Hz, 1H), 3.53 (t, 9.0 Hz, 1H), 3.87 (dd, 4.7, 10.3 Hz, 1H), 4.63–4.76 (m, 2H), 4.91 (s, 1H), 4.94 (d, 7.2 Hz, 1H), 6.4–7.4 (m, 34 H).

Phenyl 2,3-Bis-*O*-[bis(3,5-difluorophenyl)phosphino]-4,6-*O*-benzylidene-β-D-glucopyranoside, $\mathbf{L_b}$. ^1H NMR: δ 3.04 (dd, J = 4.7, 9.5 Hz, 1H), 3.12 (t, 9.1 Hz, 1H), 3.23 (t, 10.1 Hz, 1H), 3.90 (dd, 4.8, 10.3 Hz, 1H), 4.14 (m, 2H), 4.66 (d, 7.3 Hz, 1H), 4.84 (s, 1H), 6.0–7.2 (m, aromatic). ^{31}P NMR: δ 110.0 (s, 1P), 111.7 (s, 1P).

Phenyl 2,3-Bis-*O*-[bis(4-methoxyphenyl)phosphino]-4,6-O-benzylidene-β-D-glucopyranoside. ^1H NMR: δ 3.12 (s, 3H), 3.17 (s, 3H), 3.18 (s, 3H), 3.20 (s, 3H), 3.29 (t, J = 10 Hz, 1H), 3.54 (t, 10 Hz, 1H), 3.92 (dd, 10, 4 Hz, 1H), 4.51–4.55 (2 × dd, 2H), 4.58 (s, 1H), 4.59 (d, 8 Hz, 1H), 6.50–7.60 (m, aromatic). ^{31}P NMR: δ 116.59 (d, J = 3 Hz, 1P), 121.06 (d, 3 Hz, 1P).

Phenyl 2,3-Bis-*O*-[bis[3,5-bis(trimethylsilyl)phenyl]phosphino]-4,6-*O*-benzylidene-β-D-glucopyranoside. ^1H NMR: δ 0.067 (s, 18H), 0.096 (s, 18H), 0.21 (s, 36H), 3.07 (td, J = 4.8, 9.6 Hz, 1H), 3.31 (t, 10.2 Hz, 1H), 3.74 (t, 9.1 Hz, 1H), 3.92 (dd, 4.9, 10.2 Hz, 1H), 4.82 (m, 2H), 5.01 (d, 6.9 Hz, 1H), 5.08 (s, 1H), 6.2–8.2 (m, 22H). ^{31}P NMR: δ 117.8 (s, 1P), 123.6 (s, 1P).

Phenyl 2,3-Bis-*O*-[di-(4-fluorophenyl)phosphino]-4,6-*O*-benzylidene-β-D-glucopyranoside. ^1H NMR: δ 3.11 (m, 1H), 3.28 (m, 2H), 3.91 (dd, 1H, 5, 10 Hz), 4.42 (m, 2H), 4.80 (s, 1H), 4.82 (d, 1H, J = 8 Hz), 7.35–6.40 (m, 26H). ^{31}P NMR: δ 114.8 (s, 1P), 118.0 (s, 1P).

Phenyl-2,3-Bis-*O*-[bis[4-(trifluoromethyl)phenyl]phosphino]-4,6-*O*-benzylidene-β-D-glucopyranoside. ^1H NMR: δ 3.05 (m, 1H), 3.10–3.20 (m, 2H), 3.90 (dd, J = 10, 6 Hz, 1H), 4.36 (m, 2H), 4.71 (s, 1H), 4.78 (d, 7 Hz, 1H), 6.28 (d, 7 Hz, 1H), 6.60–7.40 (m, aromatic). ^{31}P NMR: δ 113.0 (s, 1P), 115.7 (s, 1P).

Phenyl-2,3-Bis-*O*-[bis(3,4,5-trifluorophenyl)phosphino]-4,6-*O*-benzylidene-β-D-glucopyranoside. ^1H NMR: δ 3.02 (m, 2H), 3.21 (m, 1H), 3.87 (m, 1H), 4.00 (m, 2H), 4.60 (d, 7.3 Hz, 1H), 4.75 (s, 1H), 6.4–7.2 (m, 18H). ^{31}P NMR: δ 110.8 (s, 1P), 111.8 (s, 1P).

Phenyl-2,3-Bis-*O*-[bis(3,5-dichlorophenyl)phosphino]-4,6-*O*-benzylidene-β-D-glucopyranoside. ^1H NMR: δ 3.02 (m, 2H), 3.24 (t, J = 9.9 Hz,

(54) The use of phosphinites for the hydrogenation of dehydro amino acids has been known since 1978: (a) Cullen, W. R.; Sugi, Y. *Tetrahedron Lett.* **1978**, 1635–1636. (b) Selke, R. *React. Kinetic. Catal. Lett.* **1979**, *10*, 135–138. (c) Jackson, R.; Thompson, D. J. *J. Organomet. Chem.* **1978**, *159*, C29-C31. (d) Selke, R.; Facklam, C.; Foken, H.; Heller, D. *Tetrahedron: Asymmetry* **1993**, *4*, 369–382. (e) Selke, R.; Schwarze, M.; Baudisch, H.; Grassert, I.; Michalik, M.; Oehme, G.; Stoll, N. *J. Mol. Catal.* **1993**, *84*, 223–237.

(55) (a) Kosolapoff, G. M.; Watson, R. M. *J. Am. Chem. Soc.* **1951**, *73*, 4101–4102. (b) Williams, R. H.; Hamilton, L. A. *J. Am. Chem. Soc.* **1952**, *74*, 5418–5420. (c) Quin, L. D.; Anderson, H. G. *J. Org. Chem.* **1966**, *31*, 1206–1209.

1H), 3.891 (dd, 4.4, 10.4 Hz, 1H), 4.02 (m, 2H), 4.59 (d, 7.2 Hz, 1H), 4.91 (s, 1H), 6.4–7.3 (m, 22H). ^{31}P NMR: δ 110.7 (s, 1P), 112.7 (s, 1P).

Phenyl-2,3-Bis-*O*-[bis(2-methylphenyl)phosphino]-4,6-*O*-benzylidene-β-D-glucopyranoside. ^{1}H NMR: δ 2.22 (s, 3H), 2.31 (s, 3H), 2.41 (s, 3H), 2.61 (s, 3H), 3.28 (td, *J* = 4.7, 9.6 Hz, 1H), 3.44 (t, 10.1 Hz, 1H), 3.61 (t, 9.2 Hz, 1H), 4.09 (dd, 4.9, 10.2 Hz, 1H), 4.67 (m, 2H), 4.97 (s, 1H), 5.03 (d, 7.3 Hz, 1H), 6.6–7.9 (m, 26H). ^{31}P NMR: δ 105.5 (s, 1P), 108.4 (s, 1P).

Phenyl-2,3-Bis-*O*-[bis(2,5-dimethylphenyl)phosphino]-4,6-*O*-benzylidene-β-D-glucopyranoside. ^{1}H NMR: δ 1.97 (s, 3H), 2.11 (s, 3H), 2.16 (s, 3H), 2.22 (s, 3H), 2.39 (s, 3H), 2.42 (s, 3H), 2.57 (s, 3H), 2.74 (s, 3H), 3.28 (td, *J* = 4.7, 9.6 Hz, 1H), 3.43 (t, 10.1 Hz, 1H), 3.69 (t, 9.2 Hz, 1H), 4.06 (dd, 4.8, 10.2 Hz, 1H), 4.78 (m, 2H), 5.03 (s, 1H), 5.09 (d, 7.3 Hz, 1H), 6.6–8.7 (m, 22H). ^{31}P NMR: δ 106.5 (s, 1P), 109.7 (s, 1P).

Preparation of Nickel Complexes. Nickel complexes were prepared from either $Ni(CO)_4$, $Ni(COD)_2$, $NiBr_2(THF)_2$, or $NiBr_2(DME)$. The salmon-colored $NiBr_2$ ether complexes form the anhydrous and relatively insoluble yellow $NiBr_2$ complex over time. The yields and purity of the reported zerovalent complexes will be substantially reduced if an appreciable amount of this insoluble $NiBr_2$ complex is present. With the exception of $NiL_a(CO)_2$ and $NiL_c(CO)_2$, the nickel dicarbonyl derivatives were characterized by $^{31}P\{^1H\}$ NMR and IR spectroscopy (Table 4) but not isolated. The bis-chelate complexes NiL_2 exist as two diastereomers as expected for tetrahedral complexes containing ligands of C_1 symmetry. The NiL(*trans*-stilbene) complexes exist as two diastereomers corresponding to coordination of opposite faces of the carbon–carbon double bond.

$NiBr_2(THF)_2$.[56] Bromine (4.160 g, 0.026 mol) was added dropwise to a slurry of nickel powder (1.500 g, 0.026 mol) in 160 mL of THF. After 2 days, the salmon-colored solids were collected by filtration and dried under a stream of nitrogen. Yield: 4.160 g (44%).

$NiBr_2(DME)$.[56] Bromine (4.160 g, 0.026 mol) was added dropwise to a slurry of nickel powder (1.500 g, 0.026 mol) in 100 mL of DME (dimethoxyethane). After 1 day, the orange slurry was heated to reflux whereupon a peach-colored solid precipitated. These solids were collected by vacuum filtration and dried under a stream of nitrogen. Yield: 7.358 g (92%).

$NiL_a(CO)_2$. To a solution of L_a (0.250 g, 0.20 mmol) in 4 mL of benzene was added a 0.60 M solution of $Ni(CO)_4$ in benzene (0.390 mL, 0.23 mmol). The solution was refluxed for 15 min. The resulting pale red solution was concentrated in vacuo. IR, ^{1}H and ^{31}P NMR spectroscopic analysis showed quantitative conversion to the dicarbonyl derivative. ^{31}P NMR: δ 137.7, 137.2 (AB, *J* = 20 Hz). ^{1}H NMR: δ 2.50 (td, *J* = 4.9, 10 Hz, 1H), 3.09 (m, 2H), 3.70 (dd, 5.1, 10.3 Hz, 1H), 4.25 (m, 2H), 4.71 (d, 6.6 Hz, 1H), 4.86 (s, 1H), 6.8–8.3 (m, 22H).

$NiL_c(CO)_2$. To a solution of L_c (0.478 g, 0.67 mmol) in 13 mL of benzene was added a 0.62 M solution of $Ni(CO)_4$ in benzene (1.082 mL, 0.67 mmol). The reaction mixture was refluxed for 30 min and then concentrated to a white solid in vacuo. Crystallization from THF/hexane afforded colorless needles. Yield: 0.451 g (81%). ^{31}P NMR: δ 139.9 (d, *J* = 32 Hz, 1P), 143.5 (d, 32 Hz, 1P). ^{1}H NMR: δ 2.88 (td, *J* = 5.0, 9.7 Hz, 1H), 3.15 (t, 9.8 Hz, 1H), 3.34 (t, 9.3 Hz, 1H), 3.83 (dd, 5.0, 10.2 Hz, 1H), 4.65 (m, 2H), 4.85 (d, 6.8 Hz, 1H), 4.96 (s, 1H), 6.7–8.0 (m, 30H).

$NiL(CO)_2$. ^{31}P NMR: **4-CH_3O** δ 141.9 (d, *J* = 34 Hz, 1P), 143.9 (d, 34 Hz, 1P); **2,5-$(CH_3)_2$** 145.2 (d, 28 Hz, 1P), 148.8 (d, 29 Hz, 1P); **4-CF_3** 138.3, 139.0 (AB, 27 Hz); **4-F** 140.5, 141.4 (AB, 31 Hz); **3,5-Cl_2** 137.1 (d, 23 Hz, 1P), 139.6 (d, 23 Hz, 1P); **2-CH_3** 143.9 (d, 29 Hz, 1P), 147.7 (d, 29 Hz, 1P); **3,5-$(TMS)_2$** 142.9 (d, 28 Hz, 1P), 147.4 (d, 29 Hz, 1P); **3,4,5-F_3** 137.8, 138.5 (AB, 24 Hz).

NiL_a(PhC≡CPh). **A.** Diphenylacetylene (0.029 g, 0.16 mmol) was added to a solution of L_a (0.201 g, 0.16 mmol) and $Ni(COD)_2$ (0.044 g, 0.16 mmol) in 4 mL of benzene. ^{1}H and ^{31}P NMR spectroscopic analysis of the orange solution showed nearly quantitative conversion to the acetylene complex with a trace of NiL_a(COD) (3%) remaining. The addition of excess diphenylacetylene afforded quantitative conversion. Dissociated COD and diphenylacetylene were removed in vacuo (100 °C, 0.001 Torr) to give the complex as an orange powder.

B. This complex was also prepared by zinc reduction of $NiBr_2(THF)_2$/L_a/PhC≡CPh in a manner analogous to the preparation of NiL_a(MVN (see below). ^{1}H NMR: δ 2.75 (td, *J* = 5.0, 9.6 Hz, 1H), 3.08 (m, 2H), 3.73 (dd, 5.0, 9.6 Hz, 1H), 4.56 (m, 3H), 4.85 (s, 1H), 6.7–8.4 (m, 32H). ^{31}P NMR: δ 141.7 (s, 1P), 142.2 (s, 1P).

$Ni(L_c)_2$. **A.** A 0.62 M solution of $Ni(CO)_4$ in benzene (0.081 mL, 0.050 mmol) was added to a solution of L_c (0.071 g, 0.10 mmol) in 5 mL of heptane and then heated to reflux for 8 h. The $Ni(L_c)_2$ complex precipitated as an orange solid upon cooling. After filtering, 0.078 g (~100%) of $Ni(L_c)_2$ was collected. ^{1}H and ^{31}P NMR spectroscopic analysis showed complete conversion to two diastereomers (~45:55).

B. The same complex was also prepared from $Ni(COD)_2$ and 2 equiv of L_c. ^{1}H NMR: δ 3.09 (m, $2H_a + 2H_b$), 3.21 (m, $4H_a + 4H_b$), 4.03 (m, $2H_a + 4H_b$), 4.39 (m, $4H_a + 2H_b$), 4.60 (d, 7.1 Hz, $2H_b$), 4.77 (d, 6.4 Hz, $2H_a$), 4.99 (s, $2H_b$), 5.10 (s, $2H_a$), 6.6–7.9 (m, $60H_a + 60H_b$). ^{31}P NMR: δ 129.2 (m, $2P_a + 2P_b$), 132.7 (m, $2P_a$), 133.7 (m, $2P_b$).

$Ni(L_a)_2$. To a solution of L_a (0.250 g, 0.20 mmol) in 20 mL of heptane was added a 0.60 M solution of $Ni(CO)_4$ in benzene (0.180 mL, 0.11 mmol). The reaction mixture was refluxed for 6 h. ^{1}H and ^{31}P NMR spectroscopic analysis showed essentially complete conversion to an approximately 50:50 mixture of two diastereomeric complexes. Upon cooling, an orange, gelatinous solid precipitated from the heptane solution. After filtering, 0.080 g (31%) of $Ni(L_a)_2$ was collected. NMR spectroscopic analyses of the solid and filtrate showed the solid enriched with one of the diastereomers (H_a below) and the filtrate with the other diastereomer (H_b). ^{1}H NMR: δ 2.09 (m, $2H_a$), 2.32 (m, $2H_b$), 2.94 (t, *J* = 10 Hz, $2H_b$), 3.11 (t, 10 Hz, $2H_a$), 3.38 (m, $2H_a + 2H_b$), 3.52 (m, $4H_a + 6H_b$), 3.67 (t, 10 Hz, $2H_a$), 4.21 (d, 7 Hz, $2H_a$), 4.73 (d, 7 Hz, $2H_b$), 5.04 (s, $2H_b$), 5.32 (s, $2H_a$), 6.6–8.7 (m, $44H_a + 44H_b$). ^{31}P NMR: δ 140.7 (m, $2P_a + 2P_b$), 143.3 (m, $2P_a + 2P_b$).

NiL_a(MVN). A solution of L_a (0.063 g, 0.050 mmol) in 1 mL of THF was added dropwise to a purple solution of $NiBr_2$(DME) (0.022 g, 0.070 mmol) in 3 mL of THF. To the resulting red-brown solution was added a solution of MVN (0.046 g, 0.25 mmol) in 1 mL of THF followed by excess Zn dust (~100 mg). After 18 h, the reaction was filtered and concentrated in vacuo. Uncomplexed MVN was removed from the crude product by vacuum sublimation (0.001 Torr, 80 °C, 2 h). The remaining solid was stirred with 20 mL of hexane for 30 min, filtered to remove an off white solid (in some cases several filtrations were necessary to completely remove the solid), and the filtrate evaporated in vacuo to an orange-brown solid. Yield was 0.064 g. This sample contained about 3% of the bis-chelate complex $Ni(L_a)_2$, however, the amount of $Ni(L_a)_2$ typically varied from 3–25%. ^{31}P NMR (C_6D_6, 25 °C, 300 MHz): δ 132.9 (s (br), ~7%), 130.5 (s (br), ~13%), 129.0 (s (br), ~16%), 127.9 (s (br), ~39%), 126.6 (s (br), 126.3 sh, ~25%). Because NiL_a(MVN) exists as a number of diastereomers which are rapidly interconverting in solution at ambient temperature the complex was further characterized by treatment with CO and by variable-temperature ^{31}P NMR spectroscopy (see Figure 5). Exposure of benzene solutions of NiL_a(MVN) to 1 atm of CO rapidly and quantitatively generated the dicarbonyl complex $NiL_a(CO)_2$ and 1 equiv of MVN as indicated by ^{1}H and ^{31}P NMR spectroscopy.

NiL_a(*trans*-stilbene). The preparation of this complex was identical to that of NiL_a(MVN) except *trans*-stilbene (0.045 g, 0.25 mmol) was used instead of MVN. Excess *trans*-stilbene was removed by vacuum sublimation under identical conditions. The orange-brown hexane filtrate was evaporated in vacuo to an orange-brown solid. Yield was 0.072 g (95%). ^{1}H and ^{31}P NMR spectroscopy showed two diastereomers (2.0:1) corresponding to coordination of opposite sides of *trans*-stilbene. ^{31}P NMR: (major) δ 124.1, 125.7 (AB, *J* = 34 Hz); (minor) 128.4, 129.5 (AB, 27 Hz). ^{1}H NMR: δ 2.66 (m, $1H_a$, minor), 2.82 (m, $1H_b$, major), 3.00–3.30 (m, $2H_a + 2H_b$), 3.70 (dd, *J* = 5.1, 10.6 Hz, $1H_a$), 3.75 (dd, 4.9, 10.3 Hz, $1H_b$), 4.20–4.40 (m, $1H_a + 1H_b$), 4.50–4.85 (m, $5H_a + 4H_b$), 4.87 (s, $1H_b$), 6.6–8.2 (m, $32H_a + 32H_b$).

NiL_c(*trans*-stilbene). To a slurry of $NiBr_2(THF)_2$ (0.026g, 0.072 mmol) in 3 mL of refluxing THF was added a solution of L_c (0.036 g, 0.050 mmol) in 1 mL of THF followed by a solution of *trans*-stilbene (0.045 g, 0.25 mmol) in 1 mL of THF. The reaction mixture was cooled to room temperature and filtered, and then zinc dust (~100 mg) was added to the burgundy filtrate. After 18 h, the reaction mixture was filtered and concentrated in vacuo. The resulting solid residue was slurried with 25 mL of hexane/diethyl ether (80/20 v/v) and filtered. Concentration of the orange filtrate in vacuo gave 0.028 g of an orange solid. ^{1}H NMR spectroscopy showed excess *trans*-stilbene in addition to the nickel complex. The ratio of the two diastereomeric nickel complexes was 1.3:1. ^{31}P NMR: δ (major) 134.8 (d, *J* = 3.5 Hz, 1P), 135.8 (d, 3.5 Hz, 1P); (minor) 140.6 (d, 7.6Hz, 1P), 142.2 (d, 7.5 Hz, 1P). ^{1}H NMR: δ 2.90 (m, 2H), 3.0–3.4 (m, 6H), 3.77 (m, 2H), 4.21 (m, 1H), 4.26 (m, 1H), 4.40 (m, 2H), 4.50 (d, 7.2 Hz, 1H), 4.75 (d, 6.4 Hz, 1H), 4.82 (s, 1H), 4.89 (s, 1H), 5.04 (m, 1H), 5.26 (m, 1H), 6.6–7.9 (aromatic H).

(56) Dr. Richard P. Beatty, DuPont Co., Experimental Station, Wilmington, Delaware 19880–0328. Unpublished results. These anhydrous nickel (II) halide/ether complexes can also be prepared directly from the hydrate complexes; see: Ward, L. G. L. *Inorg. Synth.* **1972**, *13*, 154–164.

NiL_a(COD). Ni(COD)$_2$ (0.006 g, 0.022 mmol) and L_a (0.026 g, 0.021 mmol) were stirred together in 1 mL of benzene at about 25 °C. The resulting orange solution was filtered through Celite to remove a small amount of dark solids and then evaporated in vacuo to an orange solid. Yield: 0.030 g (100%). ^{31}P NMR: δ 128.1, 127.7 (AB, J = 18 Hz). ^{1}H NMR: δ 1.4–2.2 (m, 8H), 2.62 (m, 1H), 3.20 (m, 2H), 3.78 (dd, J = 5.0, 10.4 Hz, 1H), 4.4–4.8 (m, 6H), 4.91 (d, 6.8 Hz, 1H), 4.98 (s, 1H), 6.8–8.0 (m, 22H).

NiL_c(COD). A solution of L_c (0.028 g, 0.040 mmol) in 1 mL of benzene was added dropwise to a slurry of Ni(COD)$_2$ (0.014 g, 0.051 mmol) in 0.5 mL of benzene. After 18 h, the initially orange solution darkened because of the decomposition of excess Ni(COD)$_2$. The reaction mixture was filtered through Celite and concentrated in vacuo to give 0.038 g (~100%) of an off-orange solid. ^{31}P and ^{1}H NMR spectroscopic anaylsis showed the presence of about 94% NiL_c(COD) and 6% Ni(L_c)$_2$. ^{1}H NMR: δ 1.8–2.1 (m, 8H), 3.25 (m, 2H), 3.87 (t, J = 8.5 Hz, 1H), 3.94 (m, 1H), 4.54 (m, 2H), 4.89 (m, 4H), 5.07 (s, 1H), 5.12 (d, 5.6 Hz, 1H), 6.6–8.0 (m, 30H). ^{31}P NMR: δ 135.5 (d, J = 30 Hz, 1P), 139.9 (d, 30 Hz, 1P).

General Hydrocyanation Protocol. Catalyst scouting reactions were carried out by the dropwise addition of a toluene solution of HCN (typically 0.05–1.0 equiv of HCN per equivalent of alkene) to a hexane solution of the alkene (0.1–0.2 M), Ni(COD)$_2$ (0.01–0.5 equiv), and the chiral ligand (0.01–0.05 equiv). Ligands that were insoluble in hexane were stirred separately with Ni(COD)$_2$ in benzene. The resulting catalyst solutions were evaporated to dryness and then the residue dissolved or slurried with hexane and the substrate. Hydrocyanation reactions were usually stirred at room temperature (~25 °C) overnight. The product nitriles were isolated by flash chromatography (typically 90/10 hexane/Et$_2$O, silica gel) and analyzed by ^{1}H NMR spectroscopy, MS, GC, and HPLC. Solids which formed during the course of the reaction were dissolved by adding benzene prior to isolation and analysis.

Batch reactions were carried out by premixing the solution of substrate and HCN and then rapidly adding the solution of Ni(COD)$_2$/L.

Kinetic Studies. The reaction kinetics of the NiL_a(COD) system were studied by determining the initial rates of reaction (t = 1 min, $T \approx 25$ °C) as a function of the initial HCN, MVN, and nickel concentrations. Stock solutions of the catalyst, MVN, and HCN were prepared and added using Eppendorf autopipets. Measurements of the initial MVN hydrocyanation rates were carried out by rapidly adding toluene solutions of NiL_a(COD) (0.025 M) to well-stirred toluene solutions of MVN and HCN at ambient temperature. After 1 min, 50 μL aliquots of the reaction mixture were diluted into 1 mL of cold toluene (–78 °C), thoroughly sparged with nitrogen (to remove HCN) as the solutions were warmed to room temperature, and analyzed by GC. The reaction mixtures were also analyzed by GC after 1 day to determine the final product concentration, [RCN]$_f$. For those reactions in which [HCN]$_o$ < [MVN]$_o$, [HCN]$_o$ was approximated as [RCN]$_f$.

The data shown in Figure 4 was obtained in a similar fashion by taking 50 μL aliquots from the reaction at timed intervals. Kinetic modeling of this data was carried out using MacKinetics software.[57]

Preparative Hydrocyanation of 4-Isobutylstyrene Using L_a. A mixture of L_a (0.199 g, 0.16 mmol) and Ni(COD)$_2$ (0.044 g, 0.16 mmol) were stirred in 5 mL of hexane. After 10 min, a solution of 4-isobutylstyrene (1.270 g, 7.92 mmol) in 45 mL of hexane was added. An approximately 1 M solution of HCN in toluene (11 mL, 11 mmol) was added dropwise over about 6 h and then the reaction mixture was stirred overnight. GC analysis showed complete conversion to the product nitrile. HPLC anaylsis showed a 57% ee (S). The solvents were evaporated in vacuo and vacuum transfer of the crude product using a heat gun (0.001 Torr) gave 1.10 g. A second batch of product was isolated from the nonvolatile residue by flash chromatography (90/10 hexane/Et$_2$O), yield 0.048 g, total yield 1.148 g (77%).

Preparative Hydrocyanation of MVN Using L_a. To a solution of Ni(COD)$_2$ (0.059 g, 0.22 mmol) and L_a (0.271 g, 0.22 mmol) in 10 mL of hexane was added MVN (4.00 g, 21.7 mmol) and 110 mL of hexane. An approximately 2 M solution of HCN in toluene (11 mL, 22 mmol) was added to the resulting slurry by addition funnel over 2.5 h. The initially heterogeneous solution became an orange-brown homogeneous solution about half-way through the addition and then the product precipitated as a white powder. GC anaylsis showed an 84% conversion at the end of the addition, and so an additional 3 mL of the HCN solution was added over 1 h. The reaction was stirred overnight and then benzene was added to dissolve all of the solids. GC analysis showed >99% conversion. HPLC analysis of a small sample isolated by flash chromatography (90/10 hexane/Et$_2$O) showed 84% ee. The solids which precipitated initially were enriched to 93% ee (see the section on optically pure S nitrile in the experimental section). Recrystallization provided optically pure nitrile. After concentration of the reaction mixture in vacuo, the remaining solids were slurried in 200 mL of hexane and collected by filtration, yield 3.555 g of an off-white sold. The filtrate was concentrated in vacuo to about 50 mL and a second crop of product isolated by filtration, yield 0.468 g. A third crop of product was then isolated by flash chromatographic workup of the filtrate (90/10 hexane/Et$_2$O), yield 0.380 g, total yield 4.403 g (96%).

Nickel Utility. A solution of MVN (0.120 g, 0.65 mmol) in 0.50 mL of toluene was treated with 0.013 mL of a toluene stock solution containing Ni(COD)$_2$ (0.05 M, 0.00065 mmol) and the ligand L_a (0.065 M, 0.000845 mmol). After 30 s, a 1.1 M solution of uninhibited HCN solution (1.5 mL, 1.65 mmol) in toluene was added dropwise over 10 min. GC analysis showed 55.2% conversion after 1 h and 76.9% conversion after 18 h.

Ligand Utility. To a slurry of MVN (0.460 g, 2.5 mmol) in 5 mL of hexane at room temperature was added a 0.0107 M solution of L_a in toluene (0.047 mL, 0.00050 mmol) followed by crystalline Ni(COD)$_2$ (≤0.001 g, ≤0.004 mmol) and an approximately 5 M solution of HCN (0.200 mL, 1.0 mmol) in toluene. Over a 2 day period, the HCN solution (0.200 mL) was added five more times, and after each addition, Ni(COD)$_2$ (≤0.001 g) was also added. After two days, toluene was added to dissolve the precipitated nitrile. GC and HPLC analysis of the homogeneous solution showed 88% conversion (4400 turnovers) with 84% ee.

Preparation of Optically Pure (S)-(–)-2-(6-Methoxy-2-naphthalene)-propionitrile.[58] A solution of Ni(COD)$_2$ (0.002 g, 0.007 mmol) in 1 mL of benzene was added to a solution of L_a (0.011 g, 0.0085 mmol) in 1 mL of benzene. After 30 min, the solution was added to MVN (0.120 g, 0.65 mmol) and then HCN (1.3 mL of 1.0 M in toluene, 1.3 mmol) was added. After 1 h, the mixture was concentrated to dryness and the product was isolated by column chromatography using ether/hexanes as eluant. The conversion was 85% based on the olefin and the ee was 78%. The product nitrile was recrystallized from 20 mL of boiling 10% ether/hexanes to afford 65 mg of nitrile of 89% ee. A second recrystallization afforded 28 mg of the product in greater than 99% ee as judged by HPLC analysis on the Chiracel OJ column (mp 99–100 °C; α^d_{25} = –29.4 ± 0.8°, c = 1, CHCl$_3$). Anal. C, H, N.

Competitive Hydrocyanation of MVN and 4-Fluorostyrene. Ni(COD)$_2$ (0.006 g, 0.024 mmol) was added to a solution of L_a (0.030 g, 0.024 mmol) in 5 mL of benzene. After 5 min, MVN (0.055 g, 0.30 mmol) and 4-fluorostyrene (0.037 g, 0.30 mmol) were added followed by a 1.0 M toluene solution of HCN (0.650 mL, 0.65 mmol). After 18 h, HPLC and GC analysis showed 76% ee (78% conversion) for MVN and 17% ee (30% conversion) for 4-fluorostyrene. Control reactions containing either 4-fluorostyrene or MVN gave 18% ee (86% conversion) and 76% ee (61% conversion), respectively.

Effect of Optically Enriched 2-(6-Methoxy-2-naphthalene)propionitrile on 2-Vinylnaphthalene Hydrocyanation. To a solution of 2-vinylnaphthalene (0.033 g, 0.21 mmol) and 2-(6-methoxy-2-naphthalene)propionitrile (0.034 g, 0.16 mmol, 89% ee) in 1 mL of toluene was added a 0.010 M toluene solution of Ni(COD)$_2$/L_a (0.163 mL, 0.0016 mmol) followed by a 1.0 M toluene solution of HCN (0.050 mL, 0.050 mmol). After 18 h, HPLC and GC analysis showed 66% ee [2-(2-naphthalene)-propionitrile] and 8% conversion. A control reaction run without 2-(6-methoxy-2-naphthalenyl)propionitrile gave 73% ee and 10% conversion. The same reaction run in hexane gave 70% ee and 11% conversion, as compared to 77% ee and 10% conversion for the control reaction.

DCN. Sodium spheres (0.464 g, 20 mmol) were carefully dropped into 10 mL of methanol. After the sodium was completely consumed, HCN (0.560 g, 21 mmol) was added to the solution. After 1 h, the solution was concentrated in vacuo. The resulting sodium cyanide was dried in vacuo (0.001 Torr) for 48 h.

The sodium cyanide was transferred to a three-necked round-bottom flask equiped with an addition funnel containing 3 mL of concentrated D_2SO_4, and connected to a trap containing 5 mL of toluene at –78 °C. A stream of argon was passed over the sodium cyanide and through the trap, and then the D_2SO_4 was slowly added (**Caution:** vigorous heating and bubbling occurs). Argon was passed over the reaction mixture for 1 h after the addition was complete and then the toluene/DCN solution was collected.

Deuterium Incorporation Measurements. Deuterium incorporation was measured by integration of ^{1}H NMR spectra (MVN-d_2) and/or

(57) Leipold W. S. III; McKinney, R.; Weigert, F.; Weiher, J. F. MacKinetics; 1992.

(58) The optically pure R enantiomer has been prepared via flash pyrolysis of the isocyanide; see: Wolber, E. K. A.; Ruchardt, C. *Chem. Ber.* **1991**, *124*, 1667–1672.

integration of $^{13}C\{^1H\}$ NMR (126 MHz) resonances assigned to the carbon *adjacent* to the deuterium-labeled carbon (MVN-d_2, 2-(6-methoxy-2-naphthalene)propionitrile-d_n). This latter method relies on the increased resolution of high field instruments and on the negligible NOE effect of neighboring deuterium/hydrogen atoms on the carbon resonance.[32] In the case of MVN-d_2, integration of the ^1H and $^{13}C\{^1H\}$ NMR spectra gave the same distribution of isotopomers (±2%). The H/D content of DCN was measured by hydrocyanating an excess of norbornene (0.038 g, 0.40 mmol) in 3 mL of hexane with the DCN/toluene solution (0.400 mL) in the presence of NiL_a(PhC≡CPh) (2 mL of a 0.009 M solution in hexane). After 7 h,[59] the product *exo*-2-cyanonorbornane was isolated (95/5 hexane/Et_2O; 53% isolated yield) and analyzed by GC/MS and ^1H and $^{13}C\{^1H\}$ NMR spectroscopy. The *exo*-2-cyanonorbornane contained 87% deuterium stereospecifically labeled in the 3-exo position and no deuterium enrichment of norbornene (GC/MS) was detected.

6-Methoxy-2-vinyl(2′-d_2)naphthalene, MVN-d_2. A 1.0 M solution of diisobutylaluminum hydride (24.0 mL, 24.0 mmol) in heptane was added via addition funnel to a slurry of 6-methoxy-2-naphthonitrile (4.13 g, 22.5 mmol) in 150 mL of toluene at −40 °C under a nitrogen atmosphere. After 1 h, the homogeneous solution was warmed to 0 °C and 100 mL of saturated aqueous sodium/potassium tartrate was added. After 18 h, the mixture was filtered through Celite and the aqueous layer extracted with two 50 mL portions of toluene. The organic layers were dried ($MgSO_4$) and concentrated. Flash column chromatography (90/10 hexane/Et_2O) gave 0.94 g (22%) of 6-methoxy-2-naphthaldehyde[60] as a pale yellow, microcrystalline solid.

A 2.5 M solution of *n*-BuLi (2.08 mL, 5.21 mmol) in hexane was added to a slurry of $[Ph_3PCD_3]I$ (2.168 g, 5.31 mmol) in 15 mL of THF at −20 °C under a nitrogen atmosphere. The white slurry dissolved to give an orange solution. After 1.5 h, a solution of 6-methoxy-2-naphthaldehyde (0.94 g, 5.04 mmol) in 200 mL of THF was added dropwise whereupon triphenylphosphine oxide precipitated as a white solid. After 2 days, 5 mL of acetone was added and this mixture was concentrated in vacuo. Flash column chromatography (90/10 hexane/Et_2O) gave 0.840 g (89%) of a white solid. ^1H and $^{13}C\{^1H\}$ NMR analysis showed a mixture of 92.3% d_2, 7.2% d_1, and 0.5% d_0. $^{13}C\{^1H\}$ NMR ($CDCl_3$): δ 55.2 (s), 105.8 (s), 112.5 (quintet, $J_{C\text{-}D}$ = 25 Hz, CD_2), 118.9 (s), 123.7 (s), 126.1 (s), 127.0 (s), 128.9 (s), 129.5 (s), 132.9 (s), 134.3 (s), 136.7 [s, ArCH, (for the two d_1 species: 136.80 and 136.82 ppm)], 157.7 (s). ^1H NMR ($CDCl_3$): δ 3.91 (s, 3H), 6.84 (br m, 1H, ArCH), 7.10–7.16 (m, 2H), 7.59–7.63 (m, 1H), 7.67–7.72 (m, 3H). The two d_1 species show =CH(D) resonances at 5.27 (d, 11.7 Hz) and 5.81 ppm (d, 17.6 Hz). The d_0 species shows $=CH_2$ resonances at 5.28 (dd, 0.7 Hz, 10.8 Hz) and 5.83 (dd, 0.9 Hz, 7.6 Hz).

4-(Trifluoromethyl)styrene-d_2. A 2.5 M solution of *n*-BuLi (2.30 mL, 5.75 mmol) in hexane was added to a slurry of $[Ph_3PCD_3]I$ (2.077 g, 5.10 mmol) in 10 mL of THF at −78 °C and then warmed to room temperature. After 1 h, the orange solution was cooled to −78 °C and a solution of 4-(trifluoromethyl)benzaldehyde (0.870 g, 5.00 mmol) in 3 mL of THF was added. The mixture was warmed to room temperature and, after 2 h, filtered and vacuum transferred (0.001 Torr, 25 °C). Concentration of the distillate in vacuo gave 0.596 g (69%) of a colorless liquid. ^1H NMR analysis showed the presence of a small amount of THF in addition to the alkene. The sample used in the hydrocyanation reaction was therefore purified by flash chromatography (hexane) first. ^1H NMR analysis showed 89% d_2, 10% d_1, 1% d_0 ($^{13}C\{^1H\}$ NMR analysis showed 91% d_2, 9% d_1). $^{13}C\{^1H\}$ NMR ($CDCl_3$): δ 116.0 (m, $=CD_2$, =CDH), 124.1 (q, J_{CF} = 271 Hz, CF_3), 125.5 (q, 3.7 Hz), 126.4 (s), 129.6 (q, 32.4 Hz), 135.4 [s, ArCH, (for the two d_1 species: 135.50 and 135.52 ppm)], 140.9 (s). ^1H NMR ($CDCl_3$): δ 6.74 (br m, 1H, ArCH), 7.48 (d, J = 8.5 Hz, 2H), 7.57 (d, 7.9 Hz, 2H). The two d_1 species show =CH(D) resonances at 5.36 (d, 11.0 Hz) and 5.82 (d, 18.0 Hz). The d_0 species shows $=CH_2$ resonances at 5.37 (d, 10.5 Hz) and 5.83 (d, 17.5 Hz). $^2H\{^1H\}$ NMR ($CDCl_3$): δ 5.43 (s), 5.89 (s).

4-Methylstyrene-d_2. A 2.5 M solution of *n*-BuLi (2.30 mL, 5.75 mmol) in hexane was added to a slurry of $[Ph_3PCD_3]I$ (2.077 g, 5.10 mmol) in 10 mL of THF at −78 °C and then warmed to room temperature. After 1 h, the orange solution was cooled to −78 °C and a solution of 4-methylbenzaldehyde (0.600 g, 5.00 mmol) in 3 mL of THF was added. The mixture was warmed to room temperature and, after 2 h, filtered and vacuum transferred (0.001 Torr, 25 °C). Concentration of the distillate gave 0.596 g the crude product. Flash chromatography (hexane) of a 0.230 g sample of the crude product gave 0.160 g of a colorless liquid. ^1H NMR analysis showed 92% d_2, 7.5% d_1, 0.5% d_0 ($^{13}C\{^1H\}$ NMR analysis showed 92.5% d_2, 7.5% d_1). $^{13}C\{^1H\}$ NMR ($CDCl_3$): δ 21.2 (s), 112.3 (m, $=CD_2$, =CDH), 126.1 (s), 129.2 (s), 134.8 (s), 136.5 [s, ArCH, (for the two d_1 species: 136.57 and 136.59 ppm)], 137.5 (s). ^1H NMR ($CDCl_3$): 2.38 (s, 3H), 6.71 (m, ArCH, 1H), 7.17 (d, J = 7.9 Hz, 2H), 7.35 (d, 7.9 Hz, 2H). The two d_1 species show =CH(D) resonances at 5.20 (d, 10.4 Hz) and 5.72 (d, 17.1 Hz). The d_0 species shows $=CH_2$ resonances at 5.22 (d, 10.0 Hz) and 5.73 (d, 18.0 Hz). $^2H\{^1H\}$ NMR ($CDCl_3$): δ 5.28 (s), 5.80 (s).

Hydrocyanation of MVN-d_2 with HCN. $Ni(COD)_2$ (0.016 g, 0.058 mmol) was dissolved in 4 mL of hexane, and then 1 mL aliquots were added to each of four solutions containing MVN-d_2 (0.092 g, 0.49 mmol) and $L_{a\text{-}d}$ (0.015 mmol). After 10 min of stirring, an approximately 2 M solution of HCN in toluene (0.250 mL, 0.50 mmol) was added dropwise to each solution over a period of 3 min. The solutions were stirred for 3 days and analyzed by GC, and then the product nitriles were isolated by flash column chromatography (90/10 hexane/Et_2O). Conversions and isotopic distributions are reported in the text (Table 6). $^{13}C\{^1H\}$ NMR ($CDCl_3$): δ 21.4 (m, CH_nD_{3-n}), 31.2 (s, ArCH), 55.3 (s, CH_3O), 105.6 (s), 119.5 (s), 121.7 (s), 124.9 (s), 125.3 (s), 127.9 (s), 128.7 (s), 129.3 (s), 132.0 (s), 134.0 (s), 158.1 (s). The benzylic carbon resonances were shifted upfield 0.074 ± 0.002 ppm for each deuterium present on the adjacent methyl carbon. ^1H NMR ($CDCl_3$): δ 1.68–1.71 (m, CH_nD_{3-n}), 3.92 (s, 3H), 4.00–4.04 (m, 1H, ArCH), 7.14 (d, J = 2.6 Hz, 1H), 7.19 (dd, 2.6 Hz, 9.1 Hz, 1H), 7.39 (m, 1H), 7.72–7.77 (m, 3H). ^2H NMR ($CDCl_3$) δ 1.71. The isotopomers were not resolved by ^2H NMR spectroscopy.

Similar reactions were run using 0.22 mmol of MVN-d_2, 0.30 mmol HCN, and 0.0025 mmol of NiL_a(COD) in 1 mL of THF or acetonitrile (100% conversion in both cases). Isotopic distributions were 9% d_1, 89% d_2, 2% d_3 and 13% d_1, 82% d_2, 5% d_3 for THF and acetonitrile, respectively.

Hydrocyanation of MVN with DCN. The DCN/toluene solution (0.400 mL, ~87% d) was added rapidly to a solution of MVN (0.074 g, 0.40 mmol) and NiL_a(PhC≡CPh) (2 mL of a 0.009 M solution in hexane) in a total of 3 mL of hexane. GC analysis showed 57% conversion of MVN after 18 h. Flash chromatography (90/10 hexane/Et_2O) gave 0.038 g of MVN and 0.048 g of nitrile (57% based on MVN; ee = 85% *S*). ^1H and $^{13}C\{^1H\}$ NMR spectroscopic analyses of the unreacted MVN showed 90% d_0 and 10% d_1 (see MVN-d_2 preparation for relevant spectroscopic data). ^1H, ^2H, and $^{13}C\{^1H\}$ NMR spectroscopic analysis of the nitrile showed regiospecific incorporation of deuterium in the β-methyl position with an isotopic distribution of 22% d_0, 75% d_1, 3% d_2 (see MVN-d_2 hydrocyanation for relevant spectroscopic data).

Hydrocyanation of 4-(Trifluoromethyl)styrene-d_2 and 4-Methylstyrene-d_2 with HCN. To two separate solutions of 4-(trifluoromethyl)styrene-d_2 (0.067 g, 0.39 mmol) and 4-methylstryene-d_2 (0.045 g, 0.38 mmol) in 1 mL of hexane each was added a solution of NiL_a(COD) (0.015 g, 0.011 mmol) in 1 mL of hexane, followed by a 2.0 M toluene solution of HCN (0.200 mL, 0.40 mmol). After 48 h, GC analysis showed 58% and 85% conversion of 4-(trifluoromethyl)styrene-d_2 and 4-methylstryene-d_2, respectively. Flash chromatography (90/10 hexane/Et_2O) gave 0.026 g of 2-(4-methylphenyl)propionitrile. Flash chromatography (90/10 hexane/Et_2O) followed by vacuum transfer gave 0.022 g of 2-[4-(trifluoromethyl)phenyl]propionitrile. For 2-[4-(trifluoromethyl)phenyl]-propionitrile-d_n, $^{13}C\{^1H\}$ NMR ($CDCl_3$): δ 20.8 (m, CH_nD_{3-n}), 31.0 (s, ArCH), 120.7 (s), 123.8 (quart, J_{CF} = 272 Hz, CF_3), 126.2 (quart, 13.7 Hz) 127.2 (s), 130.5 (quart, 33.3 Hz) 140.9 (s). ^1H ($CDCl_3$): δ 1.63 (m, CH_nD_{3-n}), 3.94 (m, ArCH, 1H), 7.48 (d, J = 8.4 Hz, 2H), 7.64 (d, 8.1 Hz, 2H). ^2H ($CDCl_3$): δ 1.64 (s). For 2-(4-methylphenyl)propionitrile-d_n, $^{13}C\{^1H\}$ NMR ($CDCl_3$): δ 21.0 (m, $ArCH_3$ + CH_nD_{3-n}), 30.6 (s, ArCH) 121.7 (s), 126.5 (s), 129.7 (s) 134.0 (s), 137.8 (s). ^1H ($CDCl_3$): δ 1.60 (m, CH_nD_{3-n}), 2.36 (s, 3H), 3.86 (m, ArCH, 1H), 7.19 (d, J = 7.9 Hz, 2H), 7.25 (d, 8.6 Hz, 2H). ^2H ($CDCl_3$): δ 1.58 (s).

Preparation of Authentic 2-(6-Methoxy-2-naphthalenyl)propionitrile (Enriched *S*-Enantiomer) from (*S*)-(+)-Naproxen. A 500 mL flask, equipped with an overhead stirrer, dry ice condenser vented through a bubbler and a 125 mL dropping funnel, was charged with 10.85 g (0.1 mol) of ethyl chloroformate in 100 mL of chloroform. The reaction mixture was cooled to −30 °C under nitrogen and a solution of 23.03 g (0.1 mol) of naproxen (Aldrich) and 10.12 g of triethylamine in 100 mL of chloroform was added over 40 min. The mixture was stirred at −20 to + 5 °C for 90 min. The addition funnel was replaced with a straight tube bubbler and ammonia was bubbled through the cold mixture for 20 min. After 20 min, the mixture was filtered through a buchner funnel. The solid was slurried with chloroform and filtered. The combined filtrates were washed with cold 5% NaOH solution and water, dried ($MgSO_4$),

(59) The DCN/HCN was completely consumed at this point. For comparison, hydrocyanation of MVN under identical conditions gave a 57% isolated yield of the nitrile.

(60) For an alternative preparation and characterization, see: Lee, H.; Harvey, R. G. *J. Org. Chem.* **1988**, *53*, 4587–4589.

and concentrated. A small portion of the resulting amide was recrystallized from hot ethyl acetate and was used for subsequent dehydration as outlined below.

To a solution of 1.13 g (4.93 mmol) of recrystallized naproxen amide and 2.59 g (9.86 mmol) of triphenylphosphine in 25 mL of dry 1,2-dichloroethane was added 5.5 mL of CCl_4. After 4 h of refluxing, the mixture was cooled to room temperature and concentrated. Flash column chromatography gave 0.93 g (89%) of 2-(6-methoxy-2-naphthalenyl)-propionitrile, identical in all respects to a sample described in the literature[8a] except for optical properties. HPLC analysis using a Chiralcel OB or Chiralcel OJ column (5% 2-propanol/hexane; 1 mL/min flow) showed two peaks of unequal intensity, the former being the larger component (44% ee). It is likely that some racemization may have occurred during the amide formation and/or the subsequent dehydration. The faster eluting isomer, which is the major component, was assigned as the *S*-isomer and was used for identification of the hydrocyanation product of MVN.

Preparation of Authentic 2-(4-Isobutylphenyl)propionitrile (Enriched *S*-Enantiomer) from (*S*)-(+)-Ibuprofen. (*S*)-(+)-Ibuprofen (Aldrich) was converted to the enriched *S*-enantiomer of 2-(4-isobutylphenyl)-propionitrile in a fashion analogous to naproxen (above). HPLC on a Chiralcel OJ column (0.5/99.5 i-PrOH/hexane, 0.5 mL/min) showed the larger, later eluting peak to be the *S*-enantiomer (20.3 min vs 16.6 min).

4-(Trifluoromethyl)styrene. To a slurry of $[Ph_3PCH_3]Br$ (11.78 g, 33 mmol) in 50 mL of THF at −78 °C was added a 2.5 M solution of BuLi (13.2 mL, 33 mmol) via addition funnel. The reaction mixture was warmed to room temperature and stirred for 1 h. The resulting orange solution was cooled to −78 °C and a solution of 4-(trifluoromethyl)-benzaldehyde (4.08 g, 23.4 mmol) in 15 mL of hexane was added dropwise via syringe. The reaction mixture was warmed to room temperature. After 1 h, 50 mL of acetone was added and the resulting mixture was filtered through celite and rinsed with hexane. The solvent was removed by distillation. Vacuum transfer of the residue (0.001 Torr, 25 °C) gave 1.1 g (27%) of a colorless liquid. ^{1}H NMR ($CDCl_3$): δ 5.39 (d, J = 11.0 Hz, 1H), 5.85 (d, 17.6 Hz, 1H), 6.75 (dd, 10.9, 17.6 Hz, 1H), 7.50, 7.58 (AB, 8.4 Hz, 4H).

1-Vinylnaphthalene. To a slurry of $[Ph_3PCH_3]Br$ (23.21 g, 65 mmol) in 20 mL of THF at −20 °C was added a 2.5 M solution of BuLi (25.5 mL, 64 mmol) via addition funnel. The reaction was warmed to room temperature. After 1 h, the mixture was cooled to −20 °C and 1-naphthaldehyde (9.633 g, 62 mmol) was added dropwise. The resulting solution was warmed to room temperature. After 18 h, 75 mL of acetone was added and this mixture was concentrated in vacuo. The residue was slurried with 150 mL of hexane, filtered through celite, and concentrated in vacuo. Vacuum transfer (0.06 torr) using a heat gun gave 3.70 g (39%) of a colorless oil. ^{1}H NMR (C_6D_6): δ 5.11 (dd, J = 1.7, 10.9 Hz, 1H), 5.47 (dd, 1.7, 17.3 Hz, 1H), 7.0–7.2 (m, 4H), 7.3–7.5 (m, 3H), 7.84 (m, 1H).

4-(2-Methylpropenyl)styrene. A solution of 1-bromo-2-methylpropene (6.750 g, 50 mmol) in 15 mL of THF was added dropwise to a slurry of magnesium shavings (1.337 g, 55 mmol) in 12 mL of THF (**Caution:** exothermic reaction). After 18 h, a solution of Ni(dmpe)Cl_2 (0.010 g) and 4-bromostyrene (7.322 g, 40 mmol) in 15 mL of THF was added dropwise to the Grignard solution at rate sufficient to maintain a temperature of 28–38 °C. After 18 h, the reaction mixture was decanted from residual magnesium, diethyl ether was added, and the mixture was extratcted with saturated aqueous KH_2PO_4 and water. The organic layer was dried ($MgSO_4$) and concentrated. Flash column chromatography (pentane) afforded 0.271 g of a colorless oil which was found to be pure by GC analysis.

Characterization of Product Nitriles. Product nitriles were isolated via column chromatography (90/10, hexane/Et_2O).

1-Cyanoacenaphthene. ^{1}H NMR ($CDCl_3$): δ 3.75 (ABX, J = 4.9, 17.2Hz, 1H (A)), 3.91 (ABX, 8.9, 17.2 Hz, 1H (B)), 4.63 (dd, 4.9, 9.0 Hz, 1H (X)), 7.34 (d, 7.0 Hz, 1H), 7.50–7.58 (m, 3H), 7.67–7.78 (m, 2H). MS: M^+ 179 (calcd for $C_{13}H_9N$: 179).

2-(2-Naphthalenyl)propionitrile.[8a] HPLC: OJ (95/5, 1 mL/min), 15.8, 16.8 min (major).

2-(1-Naphthalenyl)propionitrile. ^{1}H NMR ($CDCl_3$): δ 1.79 (d, J = 7.3 Hz, 3H), 4.63 (q, 7.2 Hz, 1H), 7.45–7.63 (m, 3H), 7.71 (d, 7.0 Hz, 1H), 7.85 (d, 8.3 Hz, 1H), 7.93 (t, 8.3 Hz, 2H). MS: M^+ 181.0882 (calcd for $C_{13}H_{11}N$: 181.0891).

2-(4-Phenyl-3-fluoro-2-phenyl)propionitrile. ^{1}H NMR ($CDCl_3$): δ 1.69 (d, 7.6 Hz, 3H), 3.94 (q, 7.3 Hz, 1H), 7.15–7.25 (m, 2H), 7.35–7.58 (m, 6H). ^{19}F NMR ($CDCl_3$): −116.18 (t, J = 9.4 Hz). MS: M^+ 225.0968 (calcd for $C_{15}H_{12}NF$: 225.0954). HPLC: OJ (90/10, 0.5 mL/min), 32.6 min, 34.2 min (major).

2-(4-Isobutylphenyl)propionitrile.[8a] ^{1}H NMR ($CDCl_3$): δ 0.90 (d, J = 6.6 Hz, 6), 1.63 (d, 7.3 Hz, 3H), 1.85 (sept, 6.7 Hz, 1H), 2.47 (d, 7.2 Hz, 2H), 3.87 (q, 7.3 Hz, 1H), 7.15, 7.25 (AB, 8.1Hz, 4H). MS: M^+ 187.1326 (calcd for $C_{13}H_{17}N$: 187.1360).

2-(4-Chlorophenyl)propionitrile. ^{1}H NMR ($CDCl_3$): δ 1.63 (d, J = 7.3 Hz, 3H), 3.88 (q, 7.3 Hz, 1H), 7.29, 7.37 (AB, 8.7 Hz, 4H). MS: M^+ 165.0322 (calcd for C_9H_8NCl: 165.0345). HPLC: OB(98/2, 0.5 mL/min), 18.9 min (major), 21.8 min.

2-(4-Biphenyl)propionitrile. ^{1}H NMR ($CDCl_3$): δ 1.69 (d, J = 7.3 Hz, 3H), 3.95 (q, 7.3 Hz, 1H), 7.3–7.5 (m, 5H), 7.60 (m, 4H). MS: M^+ 207.1028 (calcd for $C_{15}H_{13}N$: 207.1048). HPLC: OJ (95/5, 1.0 mL/min), 29.0 min, 38.3 min (major).

2-(4-Fluorophenyl)propionitrile. ^{1}H NMR ($CDCl_3$): δ 1.63 (d, J = 7.3 Hz, 3H), 3.89 (q, 7.3 Hz, 1H), 7.08 (m, 2H), 7.33 (m, 2H). MS: M^+ 149.0661 (calcd for C_9H_8NF: 149.0641). HPLC: OB (98/2, 0.5 mL/min), 18.9 min (major), 21.6 min.

2-(4-Phenoxyphenyl)propionitrile. ^{1}H NMR ($CDCl_3$): δ 1.85 (d, J = 7.3 Hz, 3H), 3.91 (q, 7.3 Hz, 1H), 7.0–7.5 (m, 9H). MS: M^+ 223.0995 (calcd for $C_{15}H_{13}NO$: 223.0997). HPLC: OJ (95/5, 0.7 mL/min), 29.6 min, 34.0 min (major).

2-(4-Methylphenyl)propionitrile. ^{1}H NMR ($CDCl_3$): δ 1.63 (d, J = 7 Hz, 3H), 2.36 (s, 3H), 3.88 (q, 7 Hz, 1H), 7.2–7.3 (m, 4H). MS: M^+ 145.0856 (calcd for $C_{10}H_{11}N$: 145.0891). HPLC: OB (98/2, 0.5 mL/min), 13.8 min (major), 17.3 min.

2-(4-Methoxyphenyl)propionitrile. ^{1}H NMR ($CDCl_3$): δ 1.62 (d, J = 7.3 Hz, 3H), 3.81 (s, 3H), 3.85 (q, 7.3 Hz, 1H), 6.90 (m, 2H), 7.27 (m, 2H). MS: M^+ 161.0848 (calcd for $C_{10}H_{11}NO$: 161.0841). HPLC: OB (98/2, 0.5 mL/min) 28.9 min (major), 33.5 min.

2-[4-(Trifluoromethyl)phenyl]propionitrile. ^{1}H NMR ($CDCl_3$): δ 1.68 (d, J = 7.3 Hz, 3H), 3.97 (q, 7.4 Hz, 1H), 7.49 (d, 8.1 Hz, 2H), 7.66 (d, 8.2 Hz, 2H). MS: M^+ 199.0618 (calcd for $C_{10}H_3NF_3$: 199.0607). HPLC: OB (99/1, 0.3 mL/min) 30.1 min (major), 33.2 min.

2-[4-(2-Methylpropenyl)phenyl]propionitrile. ^{1}H NMR ($CDCl_3$): δ 1.64 (d, J = 7 Hz, 3H), 1.85 (s, 3H), 1.90 (s, 3H), 3.88 (q, 7 Hz, 1H), 6.24 (s, 1H), 7.26 (m, 4H). HPLC: OJ (99/1, 0.5 mL/min) 25.8 min, 30.2 min (major).

2,3-Diphenylpropionitrile. MS: M^+ 207.1091 (calcd for $C_{15}H_{13}N$: 207.1048) ^{1}H NMR (C_6D_6): δ 2.53 (ABX, J = 6.5, 13.5 Hz, 1H), 2.66 (ABX, 8.1, 13.5 Hz, 1H), 3.28 (dd, 6.6, 8.0 Hz, 1H) 6.5–7.2 (m, 10 H).

Acknowledgment. The authors thank D. Johnson, G. Halliday, M. Beattie, E. Duvall, K. Messner, and S. Bernard for their invaluable technical assistance; C. Roe and L. Howe for multinuclear NMR and magnetization transfer studies; T. Foo, S. Kristjansdottir and, R. McKinney for many useful discussions.

Supplementary Material Available: HPLC trace of 2-(6-methoxy-2-naphthalenyl)propionitrile, $^{13}C\{^1H\}$ NMR spectra of 2-(6-methoxy-2-naphthalenyl)proprionitrile-d_n, $^{31}P\{^1H\}$ NMR spectra of NiL(*trans*-stilbene) (L = L_a, L_c), other model 2 kinetic fits, rate dependence at low HCN concentrations (11 pages). This material is contained in many libraries on microfiche, immediately follows this article in the microfilm version of the journal, and can be ordered from the ACS; see any current masthead page for ordering information.